TÜBİTAK

Turkish Journal of Earth Sciences

http://journals.tubitak.gov.tr/earth/

Research Article

Turkish J Earth Sci
(2020) 29: 1167-1188

doi:10.3906/yer-2001-9

Geochemistry, risk assessment, and Pb isotopic evidence for sources of heavy metals in stream sediments around the Ulukışla Basin, Niğde, southern Turkey

Abdurrahman LERMİ*, Emmanuel Daanoba SUNKARI
Department of Geological Engineering, Niğde Ömer Halisdemir University, Niğde, Turkey

Received: 07.01.2020 • **Accepted/Published Online:** 07.06.2020 • **Final Version:** 16.11.2020

Abstract: Concentrations of selected elements (Al, Fe, Mn, Mo, As, Cd, Cu, Cr, Ni, Co, Pb, Sb, and Zn) and Pb isotope ratios were determined in 53 sediments from Alihoca, Gümüş, Horoz, and Çakıt streams around the south-central Taurides (Ulukışla Basin), Niğde, which is a known mining province in Turkey. Several pollution and risk assessment indices were used to assess possible heavy metal pollution in the stream sediments and the associated potential ecological risks. Concentrations of As, Cd, Cu, Cr, Ni, Co, Pb, Sb, and Zn were elevated in the streams located near ancient mines, active mines, and slag piles in the area, suggesting an influence from mining activities. The pollution assessment indices indicated that the sediments were significantly polluted by As, Cd, Sb, Zn, and Pb and moderately polluted by Cu, Ni, Cr, and Co. The sediments show very high potential ecological risk with As, Cd, Sb, and Pb as the principal contributors. Ni, Cr, As, Pb, Zn, and Cd exceeded the probable effect concentrations in most of the samples implying that their concentrations may frequently affect sediment-dwelling organisms. Multivariate statistical analyses indicate that the accumulation of heavy metals in the stream sediments is due to an interplay of anthropogenic activities (mining and agrochemical application) and geogenic processes (weathering of bedrocks and supergene alteration of base metal-rich mineralization). Pb isotopic tracing indicates that total Pb in the sediments ($^{206}Pb/^{207}Pb$ = 1.09–1.29) is primarily from weathering and dissolution of ultrapotassic rocks ($^{206}Pb/^{207}Pb$ up to 1.20) and galena ($^{206}Pb/^{207}Pb$ up to 1.21) from the Pb-Zn-Au deposits in the area with some anthropogenic input from mine slag piles ($^{206}Pb/^{207}Pb$ = 1.10).

Key words: Heavy metals, stream sediments, risk assessment, Pb isotopic tracing, Ulukışla Basin, southern Turkey

1. Introduction

Stream sediments are known to be the best sampling media for assessment of heavy metal pollution in streams as they record the environmental impact on fluvial systems over time (Etler et al., 2006). Globally, the increase in anthropogenic activities such as agriculture, mining, urbanization, industrialization, transportation, and energy production, as well as geogenic processes, have caused the influx of pollutants such as heavy metals that drain into streams and rivers. Discharged heavy metals in a stream or a river system due to anthropogenic and/or geogenic inputs during the course of their transport are usually dispersed between the liquid phase and bottom sediments (Sin et al., 2001; Varol, 2011). Subsequently, geochemical processes such as adsorption, hydrolysis, and coprecipitation acting on the discharged heavy metals cause only a small fraction of metal ions to remain dissolved in water while the remaining portion settles in the sediments (Gaur et al., 2005). Heavy metals in ecological environments may accumulate in aquatic living organisms, which may finally enter into the human food chain and cause several health-related issues (Mucha et al., 2003; Varol, 2011; Omwene et al., 2018). The speciation, distribution, ecological risk, health risk, and source allotment of heavy metals have been widely studied (Vrhovnik et al., 2013; Eker et al., 2017; Jiang et al., 2017; Potra et al., 2017; Kumar et al., 2018; Pobi et al., 2019; Ustaoğlu and Tepe, 2019). Several assessment methods such as geoaccumulation index (I_{geo}), contamination factor (CF), enrichment factor (EF), pollution load index (PLI), and potential ecological risk index (RI) are used in evaluating heavy metal pollution in sediments. These methods have some constraints such as they are geochemical normalization approaches and are not adequate for evaluating the source and distribution of heavy metals in sediments (Zhao et al., 2015). Thus, there is the need to integrate and interpret the mentioned methods with multivariate statistical analysis. In this regard, factor, principal component, and hierarchical cluster analyses are widely and effectively used multivariate statistical techniques for identifying the sources of heavy metals in

* Correspondence: alermi@ohu.edu.tr

sediments (Sun et al., 2017; Das et al., 2018). However, this technique is constrained by bias in the interpretation of some source apportionment since it is incapable of identifying the contribution rates of each specific source (Yu et al., 2017).

Sediment quality guidelines (SQGs) are used to assess the level at which heavy metals in sediments may harmfully affect aquatic organisms and hence are applied in sediment quality studies (Zhang et al., 2018). The SQGs include a threshold effect concentration (TEC) and a probable effect concentration (PEC), where TEC is the chemical concentration below which no adverse biological effects occur, whereas PEC represents the chemical concentration above which adverse biological effects commonly occur (McDonald et al., 2000). Many researchers have proven that lead (Pb) isotopes are useful tracers of Pb pollution sources in sediments and contribution rates of various sources (Cheng and Hu, 2010; Lin et al., 2016; Potra et al., 2017; Orani et al., 2019). Pb in sediments usually comes from several sources including rocks, minerals, aerosols, and gasoline. Determining the total lead content of sediments can provide clues to the level of contamination but this is not enough to constrain the precise sources of contamination. In this respect, stable isotopes of Pb serve as a powerful tool for discriminating between anthropogenic and geogenic sources of Pb. In the environment, Pb exists in 4 stable isotopic forms: ^{204}Pb, ^{206}Pb, ^{207}Pb, and ^{208}Pb. Among these stable Pb isotopes, only ^{204}Pb is nonradiogenic and its abundance on earth is almost constant (Komárek et al., 2008). An integral study of Pb and other heavy metal contents in stream sediments that are polluted by industrial and mining activities is an initial approach to establishing the level of pollution. Moreover, discriminating sources of heavy metal pollution in stream sediments using the Pb isotope tracing technique serves as a good management strategy for designing pollution mitigation schemes.

The Ulukışla Basin in the Tauride belt of south-central Turkey is surrounded by streams such as Çakıt, Gümüş, Alihoca, Horoz, and Kırkgeçit (Figure 1). There are several Pb, Zn, Fe, Au, and Ag ore deposits; the majority of these deposits were exploited in ancient times, especially in Madenköy and Horoz areas (Figure 1). Some of these deposits are also currently under exploration for further plans towards exploitation. Smelting activities were common around the Gümüş and Madenköy villages, where ancient slag piles that contain high amounts of heavy metals are widespread (Lermi, 2009; Figure 1). The mines and slag piles in the area appear to pose a threat to the quality of water and sediments in the surrounding streams and rivers. Studies on heavy metal pollution in the stream sediments in the area are limited. Most of the studies were conducted to determine the heavy metal contents of the Karasu Creek (Yalcin et al., 2007, 2008a), Gümüşler Creek (Yalcin et al., 2008b), and groundwater resources (Lermi and Ertan, 2019) in the Niğde Municipality, which is not part of our study area. These studies documented evidence of heavy metal pollution in sediments and attributed it to abandoned mines along the creeks and leachate from domestic and industrial wastes. Even the groundwater resources contain very high arsenic (As) concentrations due to the prevalence of several anthropogenic activities and mixing with geothermal waters (Lermi and Ertan, 2019). There is the possibility of metal transport from the creeks and groundwater resources to the streams investigated in this study. Therefore, the aims of this study are to:

1. Determine the concentrations of 13 elements (Al, Fe, Mn, Mo, As, Cd, Cu, Cr, Ni, Co, Pb, Sb, Zn) in sediments from Çakıt, Gümüş, Alihoca, and Horoz streams around the Ulukışla Basin in Niğde.

2. Assess the level of pollution of heavy metals (As, Cd, Cu, Cr, Ni, Co, Pb, Sb, Zn) using sediment quality indicators such as enrichment factor (EF), contamination factor (CF), geoaccumulation index (I_{geo}), pollution load index (PLI), and potential ecological risk index (RI).

3. Identify the pollution sources of heavy metals using multivariate statistical analysis.

4. Discriminate the pollution sources of accumulated Pb in the sediments using Pb isotopes.

2. Materials and methods

2.1. Study area and geological setting

The Ulukışla Basin is located in Central Anatolia within the Tauride belt and covers a landmass of ~900 km^2 between the latitudes 37°30′15″ and 37°38′55″ N and longitudes 34°37′26″ and 34°59′40″ E (Figure 1). The area forms part of the central peripheral extension of the Tauride-Anatolide Platform. It is dominated by mountains with elevations ranging from 900 to 3200 m above sea level and includes major towns such as Ulukışla and Çiftehan. The area is characterized by a dry climate, considering its location in unforested heterogeneous mountains with dry steppes vegetation cover, typical of Central Anatolia (Kalelioğlu et al., 2009). The major riverine features in the area are the Gümüş, Alihoca, Horoz, and Kırkgeçit streams (Figure 1), which adjoin at the Çakıt stream and pass through Pozantı town to the Mediterranean Sea, where the samples were collected.

A wide range of rock types is exposed in the area, mostly ranging in age from Paleozoic to recent. The basement rocks are represented by Permian marble and schist (Figure 1) and tectonically overlain by Late Cretaceous Alihoca ophiolites. The Alihoca ophiolites are locally in contact with ophiolitic mélange composed of peridotite, gabbro, diabase, and diorite (Dilek et al., 1999; Lermi, 2016), which overlie the surroundings of the Alihoca and

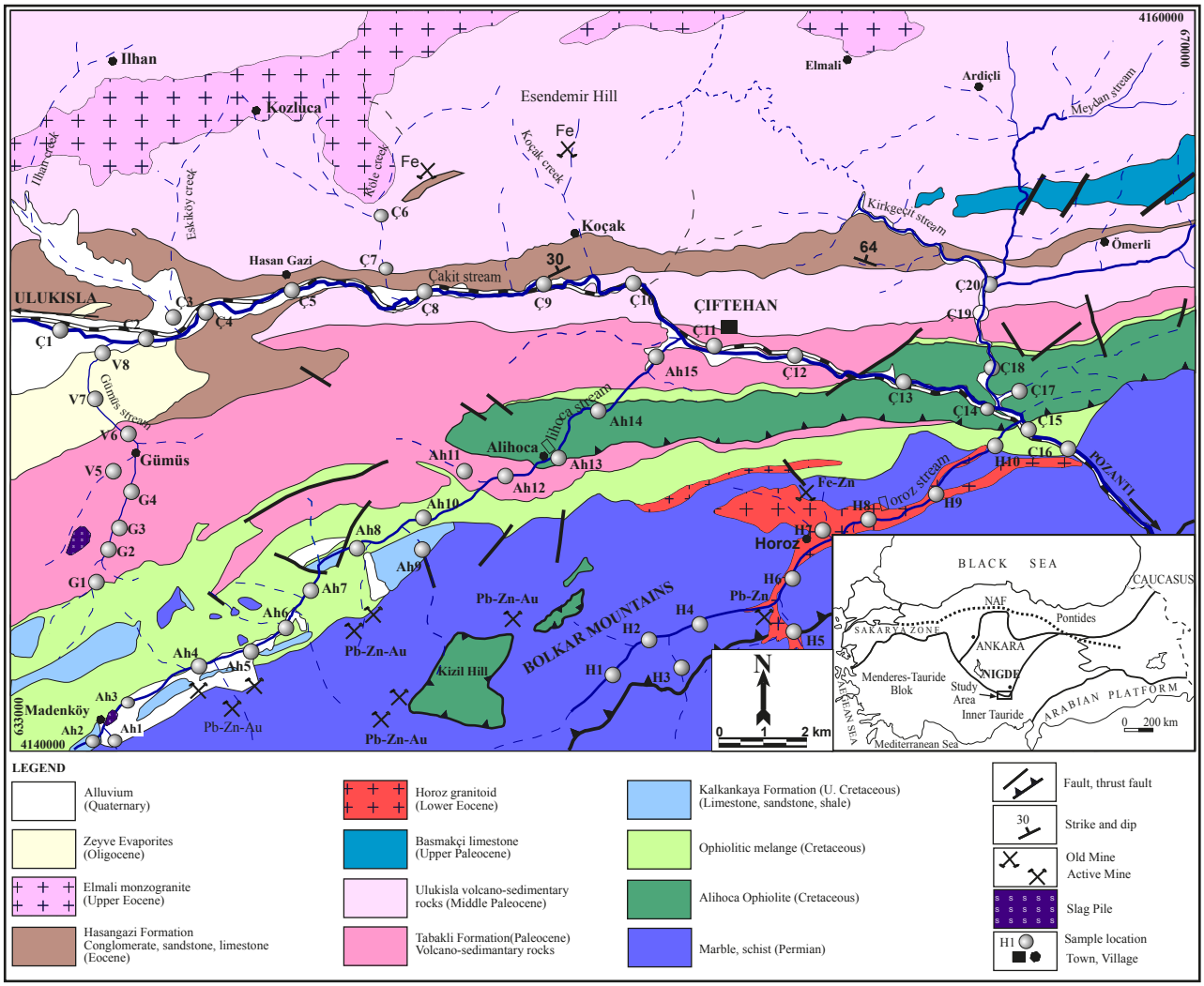

Figure 1. Simplified location and geological map of the Ulukışla Basin (modified from General Directorate of Mineral Research and Exploration – MTA maps).

Çakıt streams. The basement rocks are also intruded by the Early-Middle Eocene adakitic Horoz granitoids (Kadioglu and Dilek, 2010; Kocak et al., 2011; Kuşcu et al., 2013) in the vicinity of the Horoz stream. Locally, the Upper Cretaceous Kalkankaya Formation containing limestone, sandstone, and shale overlies the ophiolitic mélange and the basement rocks (Figure 1). The Kalkankaya Formation and most of the units are covered with Quaternary alluvial deposits towards the southwestern part of the area. The volcano-sedimentary rocks in the area are about 5 km in thickness and are dated as Late Cretaceous to Early Oligocene (Alpaslan et al., 2006), whereas volcanic rocks are approximately 2 km in thickness (Clark and Robertson, 2002). The main volcano-sedimentary units outcrop in the Early Paleocene Tabaklı Formation and Middle Paleocene Ulukışla Formation, whereas only sedimentary rocks are in the Upper Paleocene Başmakçı Formation and Early Eocene Hasangazi Formation (Figure 1). All these geological units dominate the vicinity of the Çakıt stream. The bedrock geology of the Gümüş stream is composed of volcano-sedimentary rocks (andesite, basalt, pyroclastics, limestone, and marl) of the Tabaklı Formation and Oligocene-aged Zeyve Evaporites (Figure 1).

Volcanic rocks in the area are comprised of alkaline and potassic volcanics. The alkaline volcanic rocks occur as massive lava flows and pillow lavas, whilst the potassic volcanics form dykes and massive lavas (Alpaslan et al., 2006). The majority of the alkaline volcanic rocks are intercalated with sedimentary rocks and are cut by the Upper Eocene Elmalı Monzogranite (Figure 1). The potassic volcanic rocks are mainly composed of massive lava flows and dykes, but also alternate with sedimentary rocks near the topmost part of the Middle Paleocene Ulukışla Formation. There are pockets of evaporites around

the Ulukışla area known as the Zeyve Evaporites, which are Eocene to Oligocene in age (Keskin et al., 2017; Figure 1). They cover the surroundings of the Çakıt stream. The Tauride belt of Turkey, where the Ulukışla Basin is located, hosts diverse types of ore deposits. Accordingly, the main mineral deposits in the region are Fe-Zn skarns in the contact between the Horoz granitoids and metacarbonate rocks (Kusçu, 2019), MVT- and CRD-type Pb-Zn and nonsulphide Zn deposits in carbonate rocks (Hanilçi and Öztürk, 2011; Hanilçi et al., 2019), podiform chromite in ophiolites, vein-type Sb-W-Hg-Au in the Niğde Massif (Akçay et al., 1995), bauxite, Al and Fe-rich laterite (Hanilçi, 2013; Hanilçi, 2019), and Mn deposits (Öztürk, 1997; Lermi et al., 2016). The geological units in the area are intensely deformed by small-scale thrust faults that mainly control the stream system in the area.

2.2. Sampling

A total of 53 sampling locations were sited along the Alihoca, Gümüş, Horoz, and Çakıt streams in the study area. The Çakıt stream serves as a channel for fresh sediment input from diverse sources to all streams and is linked to other streams (Figure 1). Samples were taken from the streams at the upper and lower sections, where the streams meet, to understand the dynamics of metal transport. The samples were collected from the stream channels using a spatula at a depth of 5–30 cm since the surface portions may be diluted in terms of heavy metal concentrations. The samples were then stored in self-locking polyethylene bags. They were later taken to the laboratory using ice chests and stored at room temperature to prevent cross-contamination prior to heavy metal analysis. After air-drying, they were sieved to mud-size fractions, homogenized, and pulverized to 80 µm by means of an agate mortar.

2.3. Physicochemical analysis

The total organic carbon (TOC) content of the sediments was determined by oxidation with acidified $K_2Cr_2O_7$ and back titration with ferrous ammonium sulphate, as detailed in Keskin (2012). The samples were also soaked in water with an aliquot of 10% sodium hexametaphosphate solution and gently agitated for about 1 h to enhance disaggregation. They were then washed over an 80 µm sieve and oven-dried at a temperature of 60 °C. The percent mud of the samples was calculated by multiplying the mass of the 80 µm fraction and the initial sample mass minus water content. The total carbonate content of the sediments was determined by the Bernard calcimeter method (Guitián and Carballas, 1976).

2.4. Geochemical analysis

The concentrations of 13 elements (Al, Fe, Mn, Mo, Cu, Pb, Zn, As, Cd, Sb, Co, Ni, Cr) were determined at Acme Analytical Laboratories Ltd. in Vancouver, Canada using inductively coupled plasma mass spectrometry (ICP-MS). The protocol was such that 1 g of the 80 µm fraction was digested with 6 mL HNO_3 and 2 mL H_2O_2 in a microwave digestion system. Using a 10 mL volumetric flask, the residue was diluted with deionized water. Diluted samples were filtered through a 0.45 mm filter before the analysis. Samples were analyzed in duplicates and bias was checked during the analyses. The detection limits for the 13 investigated elements are given in Table 1. Sediment reference materials, DS7 and ASH-1, treated with the same digestion method were used in the analysis to check the quality of the analysis.

2.5. Pb isotope analysis

The Pb isotopic compositions of the samples (sediments, ore minerals, and slag piles) were analyzed at Acme Analytical Laboratories Ltd. in Vancouver, Canada using a multicollector inductively coupled plasma mass spectrometry (MC-ICP-MS). The samples were digested with a mixture of aqua regia solution containing HNO_3 and HCl to determine the total and residual isotopes. Only 0.25 g sample split were analyzed. NIST-SRM-981 standard was used during the analysis to correct mass bias and dead-time effects. The standard error obtained was <0.4% RSD for the measured $^{206}Pb/^{204}Pb$, $^{207}Pb/^{204}Pb$, $^{208}Pb/^{204}Pb$, $^{208}Pb/^{206}Pb$, and $^{207}Pb/^{206}Pb$ in the sediments, whereas the ore minerals and slag piles yielded a standard error of <0.5% RSD.

2.6. Quality assurance

Reagents of guaranteed purity were used in the heavy metal concentration analysis and the acids used for digestion in the Pb isotopic analysis all contained a metal-oxide-semiconductor without impurities. All solutions were prepared using double deionized water (MILLI-Q system). Standard protocols and precautions were followed throughout the analyses. Quality control and equipment condition were guaranteed by a standard solution that was measured following every 10 samples in the heavy metal concentration analysis and every 5 samples in Pb isotopic analysis.

2.7. Metal pollution assessment

2.7.1. Enrichment factor

Enrichment factor (EF) is one of the valuable indices used in estimating the level of anthropogenic input for metal pollution in sediments. It was calculated using the equation (Grygar et al., 2014) below:

$$\mathrm{EF} = \frac{(\mathrm{C}_i/\mathrm{C}_{Al})_s}{(\mathrm{C}_i/\mathrm{C}_{Al})_b} \quad (1)$$

where $(C_i/C_{Al})_s$ and $(C_i/C_{Al})_r$ are the heavy metal/Al ratios in the samples and background, respectively. Al has been widely used for geochemical normalization because of its conservative nature (Ettler et al., 2006). The background values correspond to metal contents in the average shale (Table 1), as presented in Turekian and Wedepohl (1961);

Table 1. Concentrations and statistical summaries of heavy metals and physicochemical parameters in the sediments of the Ulukışla Basin. (All heavy metals are measured in mg/kg whereas all physicochemical parameters of Al, Fe are measured in %; AS: Average Shale from Turekian and Wedepohl, 1961.)

Sample	Al	Fe	Mn	Mo	Cu	Pb	Zn	As	Cd	Sb	Co	Ni	Cr	TOC	Mud	$CaCO_3$
DL	0.02	0.02	2.00	0.01	0.02	0.01	0.20	0.20	0.02	0.04	1.00	1.00	1.00	0.02		0.02
Ah1	3.08	2.23	1121	0.89	79	13	174	5	0.28	1.70	19	134	155	2.50	46	33
Ah2	1.93	3.73	738	0.90	42	12	58	16	0.24	0.71	26	153	81	0.75	35	14
Ah3	2.00	3.57	693	0.84	49	11	97	25	0.42	1.05	29	199	141	0.90	39	12
Ah4	0.72	4.47	943	22.71	984	605	2215	4361	3.02	51	13	170	98	4.62	52	37
Ah5	1.28	2.63	923	5.85	252	163	953	1285	3.60	97	23	279	189	3.41	48	34
Ah6	1.23	3.24	714	3.10	106	40	444	593	1.47	28	36	550	298	2.10	30	25
Ah7	1.51	3.56	810	2.64	88	40	307	350	1.00	22	51	680	375	1.70	35	22
Ah8	0.81	2.85	997	2.86	62	16	999	347	6.68	11	24	293	206	1.20	25	31
Ah9	0.52	3.51	1559	10.53	96	46	3103	1061	18.91	29	17	164	146	2.62	20	48
Ah10	0.53	2.08	778	4.26	46	12	708	287	5.16	13	16	182	107	0.92	20	56
Ah11	0.54	2.32	887	5.18	62	20	942	439	5.86	18	17	186	118	1.27	35	52
Ah12	0.52	2.22	732	3.51	64	10	781	286	6.15	9.00	14	148	85	0.63	30	53
Ah13	0.42	2.45	770	6.62	85	19	1295	483	8.31	17	15	146	85	0.95	17	57
Ah14	0.50	2.12	715	2.43	33	14	286	100	2.07	3.85	16	206	124	0.60	19	50
Ah15	0.40	2.70	815	7.16	51	17	655	342	4.47	12	24	235	138	1.12	16	49
Ç1	0.81	2.85	997	2.86	62	16	87	6.3	2.35	11	24	293	206	0.50	20	45
Ç2	1.67	3.44	699	0.47	38	162	65	37	0.45	1.51	32	340	208	0.60	38	37
Ç3	0.78	2.89	886	3.12	72	13	122	4.3	4.65	11	22	291	209	0.85	26	35
Ç4	2.37	4.10	709	0.22	48	49	68	10	0.31	0.30	35	346	192	1.32	23	33
Ç5	1.38	3.04	910	0.69	31	119	77	25	0.34	1.36	20	199	119	2.40	30	43
Ç6	1.72	3.65	673	0.45	40	54	67	11	0.39	0.60	30	346	179	0.74	36	35
Ç7	2.25	3.51	1068	0.41	32	46	63	9.0	0.23	0.43	20	157	90	0.64	24	28
Ç8	1.61	3.17	832	0.57	34	146	58	43	0.34	1.95	24	227	137	2.13	45	32
Ç9	1.53	3.19	807	0.40	34	29	49	10	0.33	0.36	24	259	142	0.90	32	43
Ç10	1.26	3.09	574	0.29	25	55	50	15	0.27	0.68	19	154	81	0.84	36	25
Ç11	1.57	2.60	779	0.51	26	82	92	19	0.20	0.73	21	199	121	0.60	43	35
Ç12	1.74	3.18	737	0.20	31	82	53	11	0.21	0.52	40	543	372	0.98	46	18
Ç13	1.39	2.24	536	1.27	30	13	164	49	0.99	1.50	20	245	125	1.70	56	37
Ç14	0.43	2.17	687	4.33	46	7	503	201	4.01	8.35	20	199	109	2.25	46	50
Ç15	1.95	3.06	556	1.22	45	13	222	63	1.52	2.35	24	216	155	0.80	36	22
Ç16	1.27	2.58	644	2.98	47	16	96	153	3.13	5.96	23	200	131	1.40	35	38
Ç17	2.05	3.24	693	0.25	36	20	62	5.8	0.27	0.29	24	167	94	0.87	42	28
Ç18	1.01	2.49	633	19.71	116	12	56	50	6.38	5.41	10	56	205	1.95	21	44
Ç19	1.34	2.35	735	0.34	28	120	58	16	0.55	1.35	22	206	100	0.75	33	34
Ç20	1.57	2.82	894	0.29	34	165	58	27	0.39	1.22	29	269	150	1.10	35	30
G1	0.95	2.53	650	1.01	20	34	36	10	0.54	0.44	24	367	176	0.40	20	59
G2	0.87	2.36	593	1.02	21	63	47	12	0.53	0.63	24	334	161	0.60	15	57
G3	1.10	2.53	580	0.88	22	48	38	10	0.47	0.46	26	340	186	0.50	45	50
G4	1.52	3.26	701	2.00	48	1288	110	284	0.63	15	30	368	249	0.98	53	31

Table 1. (Continued).

G5	1.29	2.80	677	1.01	29	332	76	97	0.55	2.99	28	374	210	0.65	40	43
G6	1.04	2.56	632	1.47	31	247	49	163	0.58	4.67	25	346	191	1.95	35	51
G7	2.17	3.85	699	0.22	46	96	74	15	0.44	0.56	30	304	159	1.25	57	33
G8	2.03	3.60	689	0.26	42	39	57	9.6	0.38	0.45	30	281	155	0.65	45	43
H1	0.50	1.60	291	0.79	6.5	22	268	7.7	0.42	0.34	7.13	31	51	0.85	22	48
H2	0.53	4.80	387	0.80	9.0	14	57	8.9	0.41	0.49	7.70	37	47	0.44	19	46
H3	0.14	3.40	669	0.75	14	24	193	7.3	0.36	0.35	0.50	52	72	0.55	7.9	32
H4	0.10	3.41	617	20.21	24	74	112	219	0.49	12	11	29	36	3.25	14	38
H5	0.60	3.52	291	5.21	15	58	403	74	0.42	2.31	10	15	18	2.40	51	26
H6	0.46	3.35	552	2.76	7.1	34	110	125	0.45	3.60	5.26	31	28	1.62	45	40
H7	0.38	4.33	359	2.35	8.9	134	163	12	0.34	0.43	6.41	25	32	0.95	26	37
H8	0.12	2.75	469	2.55	16	68	81	7.4	0.29	0.35	10	39	48	0.60	10	30
H9	0.31	4.86	492	9.37	13	30	97	29	0.35	1.16	6.70	21	29	1.15	17	27
H10	0.44	1.87	314	3.79	11	13	64	7.6	0.24	0.23	6.70	33	37	1.35	19	32
AS	8.80	4.70	850	6.20	45	20	90	13	0.30	1.50	20	68	90			
Min.	0.10	1.60	291	0.20	6.48	6.89	36	4.30	0.20	0.23	0.50	15	17.8	0.40	7.90	12.41
Max.	3.08	4.86	1559	22.71	984	1288	3103	4361.3	19	97	51	680	375	4.62	57	59
Mean	1.14	3.03	715	3.33	63	91.94	323	223	1.94	7.89	21	220	139	1.30	32	38
Median	1.10	3.04	699	1.27	36	39	96	27	0.47	1.51	22	200	137	0.95	35	37
Std. Dev.	0.68	0.72	219	4.94	135	194	558.6	631	3.17	16	9.65	142	78	0.87	13	11
Kurtosis	–0.25	0.18	3.45	7.73	44	29	13	37	15	21	0.83	1.33	1.63	3.41	–0.98	–0.49
Skewness	0.51	0.53	0.88	2.76	6.46	5.04	3.394	5.75	3.41	4.14	0.33	0.81	0.95	1.73	0.09	–0.02

the same background values were used for calculations of other indices. The average shale was used since the bedrock geology of the streams is different and all the streams are affected by pollution from different sources. In addition, most sediment quality studies have used the metal contents in the average shale for background values due to similar reasons (Zhang et al., 2016; Kumar and Singh, 2018). The 5-class pollution categorization of Andrews and Sutherland (2004) on the basis of EF values was used in the metal pollution evaluation, where EF < 2 indicates minimal pollution; EF 2–5 indicates moderate pollution; EF 5–20 indicates significant pollution; EF 20–40 indicates high pollution; EF > 40 indicates extreme pollution.

2.7.2. Geoaccumulation index

The level of metal pollution in the sediments was evaluated by the geoaccumulation index (I_{geo}), initially presented by Müller (1969). The I_{geo} values were calculated from the following equation:

$$I_{geo} = \log_2\left[\frac{C_n}{1.5B_n}\right] \quad (2)$$

where C_n is the metal (n) concentration (mg/kg) and B_n denotes the background concentration of that metal (n) (mg/kg). The coefficient 1.5 is used to explain the likely variations in the background values as a result of lithogenic input (Müller, 1969). Seven classes have been established for the I_{geo} values: class 0 ($I_{geo} \leq 0$), practically unpolluted; class 1 ($0 < I_{geo} < 1$), unpolluted to moderately polluted; class 2 ($1 < I_{geo} < 2$), moderately polluted; class 3 ($2 < I_{geo} < 3$), moderately to heavily polluted; class 4 ($3 < I_{geo} < 4$), heavily polluted; class 5 ($4 < I_{geo} < 5$), heavily to extremely polluted; class 6 ($I_{geo} > 5$), extremely polluted (Müller, 1981).

2.7.3. Contamination factor

Contamination factor (CF) is the ratio of the individual metal contents in sediments and the background value (equation 3; Hakanson, 1980).

$$\mathrm{CF} = \frac{C_{heavy\ metal}}{C_{background}} \quad (3)$$

The CF values obtained from equation 3 in this study were interpreted using the scheme of Hakanson (1980) where: CF < 1 indicates no or low contamination; 1 ≤ CF < 3 indicates moderate contamination; 3 ≤ CF < 6 indicates considerable contamination; and CF ≥ 6 indicates very high contamination.

2.7.4. Pollution load index

The pollution load index (PLI) was estimated from CFs in equation 4 (Tomlinson et al., 1980).

$$PLI = (CF_1 \times CF_2 \times CF_3 \times ... \times CF_n)^{1/n} \quad (4)$$

The numerical values obtained from equation 4 above provided a simple conceptual way of evaluating metal pollution in the sediments. If PLI > 1, it indicates that the sediments are polluted, and if PLI < 1, then there is no metal pollution (Tomlinson et al., 1980).

2.7.5. The potential ecological risk index

The potential ecological risk index (RI) was initially proposed by Hakanson (1980). The RI was calculated from the equations below:

$$E_r^i = T_i \times C_i/B_i \quad (5)$$

where C_i represents the concentration of the metal in the sediment, B_i is the background value of the metal *i* in the average shale, and T_i is the normalized toxic coefficient of metal *i*; values of all the studied metals in mg/kg (As = 10; Cd = 30; Cu, Co, Ni, Pb = 5; Hg = 40; Zn = 1; Cr = 2) were taken from Hakanson (1980).

$$RI = \sum_{i=1}^{n} E_r^i \quad (6)$$

where E_r^i repres ents the potential ecological risk factor of each heavy metal.

2.8. Multivariate statistical analyses

In this study, Pearson's correlation matrix (PCM) was used to identify the possible relationships that exist among the heavy metals. R-mode Factor Analysis (FA) was employed in ascertaining the sources of sediment pollution (geogenic and anthropogenic). It was done by generating several factors that represent a group of interconnected variables in the dataset. Principal component analysis (PCA) was the extraction method used during the R-mode FA, and varimax rotation was the chosen mode of displaying the factors. Kaiser (1960) criterion was applied to reduce the extracted factors to 3 with eigenvalues > 1 since several factors are usually extracted in the R-mode FA (Sunkari et al., 2019; Zango et al., 2019). Hierarchical cluster analysis was used to identify the element associations. All these analyses were done in SPSS version 22 (IBM Corp., Armonk, NY, USA).

3. Results and discussion

3.1. Physicochemical parameters in the sediments

The concentrations of the physicochemical parameters and statistical summaries are given in Table 1. The TOC varies from 0.40%–4.62% with a mean of 1.30% in all 53 samples collected from the 4 streams (Table 1). Samples from Alihoca stream show the highest TOC content (0.60%–4.62%), followed by samples from Horoz stream (0.44%–3.25%), whereas the lowest TOC contents are observed in those from Çakıt stream (0.50%–2.40%) and Gümüş stream (0.40%–1.95%). The highest TOC contents (4.62% and 3.25%) were observed in samples Ah4 and H4, respectively, in close proximity to Pb-Zn-Au deposits in Madenköy and Horoz villages (Figure 1). This may be due to sediment gangue-derived carbonate minerals around the Alihoca and Horoz streams. The mud contents of the sediments vary from 7.90%–56.5% (mean of 32.1%) with the maximum at sample point C13 in the Çakıt stream, and may be due to spring tide (Liu et al., 2018) both below and above the Çakıt streambed. The Çakıt stream is a major conduit for fresh terrestrial sediments from other sources in the area and serves as a source of a sink system that links the Gümüş, Alihoca, and Horoz streams (Figure 1). Thus, the higher mud content observed is a result of fresh sediment input from the source(s) of the Çakıt stream. The $CaCO_3$ content ranges from 12%–59.3% (mean of 37.6%) with the maximum at sample point G1 along the Gümüş stream, indicating the presence of carbonates in the sediments. The abundance of carbonate sedimentary rocks in the Tabaklı Formation that overlay the vicinity of the Gümüş stream is consistent with this conclusion. The $CaCO_3$ content might be controlled by the supply of excess Ca^{2+} into the streams from the surrounding rivers and also a function of intense weathering of Ca-bearing silicate minerals like plagioclase, pyroxene, amphibole, and chlorite (Hanken et al., 2015).

3.2. Heavy metal concentrations in the sediments

Concentrations and statistical summaries of Mn, Fe, Al, and heavy metals in the sediments are presented in Table 1. The mean concentrations (mg/kg) vary in the order of Mn (715) > Zn (323) > As (223) > Ni (220) > Cr (139) > Pb (92) > Cu (63) > Co (21) > Sb (7.9) > Mo (3.3) > Fe (3.0%) > Cd (1.9) > Al (1.1%). Mo, Cu, Zn, As, Cd, Sb, Co, Ni, and Cr present the highest concentrations in the Alihoca stream, whereas Fe and Pb present the highest concentrations in the Horoz and Gümüş streams, respectively. However, the Çakıt stream contains the lowest concentrations of all the investigated heavy metals in the sediments. This observation is likely because the other streams are all tributaries of the Çakıt stream and metals in the Çakıt stream may deposit into sediments in the adjoining Gümüş, Alihoca, and Horoz streams due to the high tides in the streambeds and recurrent material swapping between the water and underlying sediments. The concentration of most heavy metals in the sediments is significantly larger in the mining districts, especially in the Gümüş and Horoz villages, where Pb-Zn-Au, Fe-Zn deposits and old mines are dominant. Therefore, the heavy metal enrichment in these areas is due to hydromorphic or fluvial dispersion from the surrounding deposits. Nevertheless, towards the Kırkgeçit stream in the eastern fringe of the study area, there are no known deposits or mines, but some samples collected from the adjoining Çakıt stream in this area have high heavy metal concentrations. High concentrations of Mo (0.3–19.7 mg/kg), Cu (28–116 mg/kg), Pb (12–165 mg/kg), As (16–50 mg/kg), Cd (0.39–6.38 mg/kg), and Sb (1.22–5.41 mg/kg) for samples Ç18, Ç19, and Ç20 may

give implications for a hidden mineralization around the Kırkgeçit stream. Therefore, this location requires careful geochemical reevaluation to validate this finding.

The heavy metal concentrations of the sediments in this study can be compared to several studies of stream and river sediments in other countries and within Turkey (Table 2). In south-central Turkey, several researchers have documented evidence of heavy metal pollution in various streams and creeks (e.g., Demirak et al., 2006; Tuna et al., 2007; Yalcin et al., 2007; Yalcin et al., 2008a, 2008b; Eker et al., 2017). These studies mostly point to mining and industrial activities as the dominant source of heavy metals in streams. For instance, Eker et al. (2017) stated that sediments in the Ankara stream are extremely polluted with As, Ni, Pb, and Cd due to industrial activities. This exposes the Ankara stream to severe ecological risk. Similarly, Tuna et al. (2007) reported elevated contents of heavy metals, especially Cu, Pb, Zn, Cr, Co, and Mn in the Saricay stream. They attributed the heavy metal pollution to industrial point sources. Tuna et al. (2007) also mentioned that the seasonal trend of the heavy metals in the Saricay stream can be explained by the influence of wastewaters that lead to accumulation of high amounts of heavy metals in the dry season, and by agricultural activities that release compounds containing heavy metals into the stream. It is, however, worrying to note that the stream sediments around the Ulukışla Basin in the current study present higher values for most of the heavy metals when compared with these studies.

3.3. Pollution assessment of heavy metals

Elements such as Al, Fe, Mn, and Mo were not included in pollution assessment since they pose negligible threats to sediment quality and sediment-dwelling organisms. However, Cu, Pb, Zn, As, Cd, Sb, Co, Ni, and Cr were used in the pollution assessment. The means of EF values vary in the order of As > Cd > Sb > Zn > Pb > Cu > Ni > Cr (Figure 2a). The EF values of heavy metals in the sediments were As (1.0–4100), Cd (2.7–1067), Sb (0.7–662), Zn (2.7–583), Pb (1.5–373), Cu (2.7–267), Ni (5.6–76), Cr (2.9–51), and Co (1.6–37). Such concentrations suggest moderate to severe enrichment. Zhang and Liu (2002) indicated that EF values between 0.5 and 1.5 usually imply that heavy metals are mainly from crustal or geogenic sources, whereas EF values above 1.5 largely point to anthropogenic sources for heavy metals. In this study, the mean EF values for all the studied metals are above 1.5, suggesting an intense anthropogenic impact on the total heavy metal load in the sediments. The highest EF values for As, Cd, Zn, Cu, and Ni; Sb, Cr, and Co; and Pb are observed in Alihoca, Horoz, and Gümüş streams, respectively. However, Çakıt stream shows the lowest EF values for all the studied heavy metals. This trend is expected because there are several active Pb-Zn-Au mines around the vicinity of Alihoca and Horoz streams (Figure 1) and high EF values are due to metallic wastewater discharges from the mines. However, the highest EF value for Pb observed in the Gümüş stream is likely the result of slag piles from old mineral processing activities in the Gümüş village, where the ore was exploited from Madenköy village (Figure 1). The absence of active and old mines around the Çakıt stream might account for low EF values, and thus agricultural and domestic activities may account for high EF values in some of the samples. Total EF values for the streams vary in the order of Alihoca stream > Horoz stream > Gümüş stream > Çakıt stream.

Table 2. Comparison of the mean concentrations of measured heavy metals in the stream sediments of this study with those reported for other streams and rivers from different countries and within Turkey.

Locations	Mean Concentrations (mg/kg)								References
	As	Cd	Cr	Cu	Ni	Pb	Sb	Zn	
Ulukisla-Çiftehan streams, Turkey	223.4	1.9	138.8	62.9	220.1	91.9	7.9	323	This study
Ankara stream, Turkey	16.4	0.2	-	32.2	67.9	17.6	-	111	Eker et al. (2017)
Pazarsuyu stream, Turkey	-	0.16	10.7	17.8	-	19.7	-	32.7	Ustaoğlu and Tepe (2019)
Moryayla (Erzurum) stream sediments, Turkey	25.2	-	18.8	82.2	17.6	31.2	0.7	101.1	Kirat and Aydin (2018)
Mustafakemalpasa stream, Turkey	154	8.78	516	26.2	274	65.6	-	110	Omwene et al. (2018)
Gümüşler creek, Niğde, Turkey	268.6	4.4	496.4	26.2	28.3	49.1	154.6	64.8	Yalcin et al. (2008a)
Mount Pinatubo-Dizon Mine area, the Philippines	0.40	0.02	32.3	22.85	14.3	1.39	0.03	33.6	Zuluaga et al. (2017)
Sediments of Jinjiang river estuary, China	-	1.59	99.9	102	28.5	95.6	1.93	331	Yu et al. (2017)
West Xiamen Bay, China	-	-	74.9	52.5	-	37.5	-	258	Yang et al. (2016)
Gironde Estuary, France	18.7	0.48	78.4	24.5	-	46.8	-	168	Larrose et al. (2010)
Masan Bay, Korea	-	1.24	67.1	43.4	-	44	-	206.3	Hyun et al. (2007)
Buriganga river, Bangladesh	-	3.3	178	28	200	70	-	-	Ahmad et al. (2010)
Gomti river, India	-	2.42	8.15	5	15.7	40.3	-	-	Singh et al. (2005)

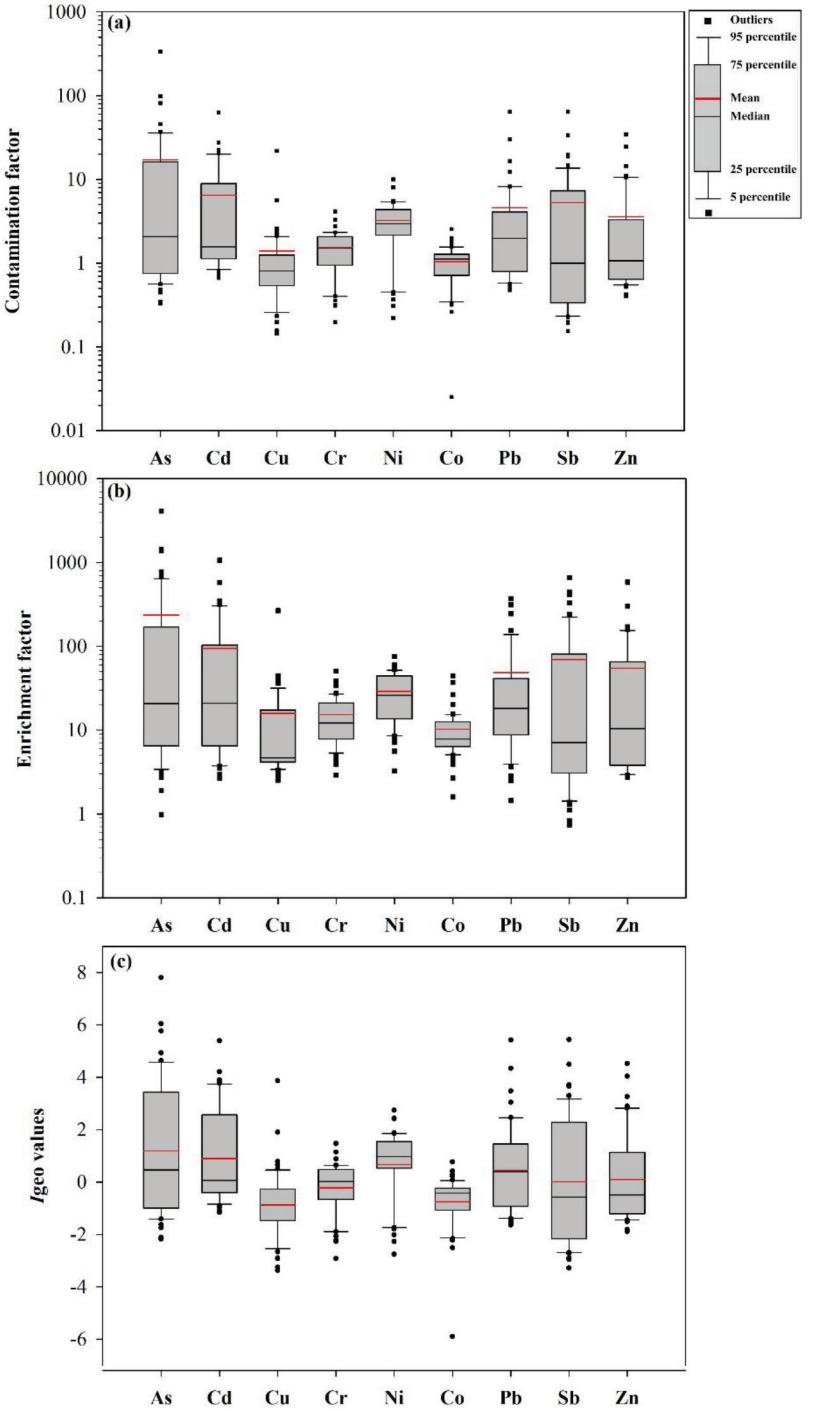

Figure 2. Box and whisker plots for (a) enrichment factors, (b) I_{geo} values, and (c) contamination factors of heavy metals (As, Cd, Cr, Cu, Ni, Pb, Sb, Zn) in sediments of the Ulukışla Basin.

The I_{geo} values of the studied heavy metals range from As (–1.2–7.8), Cd (–1.2–5.4), Zn (–1.9–4.5), Sb (–3.3–5.4), Pb (–1.6–5.4), Cu (–3.4–3.9), Ni (–2.3–2.7), Cr (–2.9–1.5), and Co (–5.9–0.8) (Table 3). The I_{geo} values followed the order As > Cd > Zn > Sb > Pb > Cu > Ni > Cr (Figure 2b). The highest I_{geo} values of the metals were found in samples from Alihoca and Gümüş streams. The I_{geo} values of As, Cd, Pb, and Sb permit them to be classified as "extremely polluted" for most samples collected from the Alihoca and Gümüş streams. Accordingly, the samples with I_{geo}

Table 3. Sediment contamination assessed by CF, EF, I_{geo}, PLI, and RI in the Ulukışla Basin (n = 53).

Element		Cu			Pb			Zn			As			Cd			Sb			Co			Ni			Cr				
Stream		CF	EF	I_{geo}	CF	EF	I_{geo}	CF	EF	I_{geo}	CF	EF	I_{geo}	CF	EF	I_{geo}	CF	EF	I_{geo}	CF	EF	I_{geo}	CF	EF	I_{geo}	CF	EF	I_{geo}	PLI	RI
Alihoca	Min.	0.7	4.3	−1.0	0.5	1.5	−1.6	0.6	2.9	−1.2	0.3	1.0	−2.1	0.8	2.7	−0.9	0.5	2.2	−1.7	0.6	2.7	−1.3	2.0	5.6	0.4	0.9	4.1	−0.7	0.8	68.6
	Max.	21.9	267.3	3.9	30.3	369.8	4.3	34.5	583.4	4.5	335.5	4100.4	7.8	63.0	1066.7	5.4	64.8	445.2	5.4	2.6	26.4	0.8	10.0	75.9	2.7	4.2	33.7	1.5	6.0	4298.2
	Mean	3.1	36.0	0.3	3.4	39.4	−0.2	9.6	140.8	2.0	51.2	648.7	3.6	15.0	237.4	2.5	14.0	160.4	2.2	1.1	12.0	−0.5	3.7	39.4	1.1	1.7	18.6	0.1	2.6	1172.7
	Median	1.4	16.8	−0.1	0.8	12.2	−0.8	7.9	120.6	2.4	26.7	366.2	4.2	12.0	123.0	3.0	8.8	134.2	2.5	0.9	12.9	−0.7	2.7	44.5	0.9	1.5	19.8	0.0	2.5	873.7
Çakıt	Min.	0.6	2.7	−1.4	0.5	2.9	−1.5	0.5	2.7	−1.5	0.3	1.9	−2.2	0.7	3.0	−1.2	0.2	0.7	−3.0	0.5	3.9	−1.6	0.8	7.2	−0.9	0.9	3.9	−0.7	0.6	63.5
	Max.	2.6	22.4	0.8	8.3	46.3	2.5	5.6	114.4	1.9	15.5	316.3	3.4	21.3	273.6	3.8	7.4	113.9	2.3	2.0	20.3	0.4	8.0	59.9	2.4	4.1	26.2	1.5	1.9	740.1
	Mean	0.9	7.2	−0.8	3.1	18.2	0.4	1.2	11.2	−0.7	2.9	29.4	0.1	4.6	45.6	0.6	1.9	19.5	−0.6	1.2	8.0	−0.4	3.6	24.2	1.1	1.7	11.9	0.1	1.1	233.7
	Median	0.8	4.3	−0.9	2.4	11.5	0.7	0.7	4.1	−1.0	1.4	8.2	−0.1	1.3	7.3	−0.2	0.9	5.5	−0.7	1.2	6.8	−0.4	3.3	20.1	1.1	1.6	8.9	0.0	1.1	138.5
Gümüş	Min.	0.5	3.9	−1.7	1.7	8.5	0.2	0.4	2.7	−1.9	0.7	3.2	−1.0	1.3	5.5	−0.2	0.3	1.3	−2.4	1.2	6.1	−0.3	4.1	17.9	1.5	1.7	7.2	0.2	0.8	95.0
	Max.	1.1	6.2	−0.5	64.4	372.8	5.4	1.2	7.1	−0.3	21.9	126.5	3.9	2.1	17.9	0.5	10.1	58.4	2.7	1.5	12.1	0.0	5.5	50.0	1.9	2.8	18.1	0.9	2.5	751.1
	Mean	0.7	4.7	−1.1	13.4	85.7	2.0	0.7	4.5	−1.2	5.8	39.1	0.6	1.7	12.4	0.2	2.1	13.8	−0.8	1.3	9.3	−0.2	5.0	36.0	1.7	2.1	14.6	0.4	1.3	237.4
	Median	0.7	4.3	−1.2	4.0	25.7	1.4	0.6	4.2	−1.4	1.0	8.0	−0.6	1.8	12.5	0.2	0.4	3.5	−1.9	1.3	9.9	−0.2	5.0	38.8	1.8	2.0	16.3	0.4	0.9	120.7
Horoz	Min.	0.1	2.5	−3.4	0.6	11.7	−1.2	0.6	10.6	−1.2	0.6	10.4	−1.4	0.8	15.9	−0.9	0.2	3.1	−3.3	0.0	1.6	−5.9	0.2	3.3	−2.8	0.2	2.9	−2.9	0.5	41.3
	Max.	0.5	44.7	−1.5	6.7	313.7	2.2	4.5	136.3	1.6	16.8	1435.0	3.5	1.6	137.9	0.1	7.8	662.3	2.4	0.5	44.8	−1.5	0.8	48.8	−1.0	0.8	50.7	−0.9	1.4	322.7
	Mean	0.3	12.1	−2.6	2.3	95.0	0.3	1.7	54.6	−0.1	3.8	189.8	0.1	1.3	45.6	−0.3	1.4	80.4	−1.4	0.4	13.2	−2.4	0.5	18.3	−1.8	0.4	17.7	−1.9	0.7	109.7
	Median	0.3	4.7	−2.5	1.6	42.7	0.1	1.2	47.0	−0.3	0.8	38.4	−0.9	1.3	27.3	−0.2	0.3	15.9	−2.3	0.3	7.0	−2.1	0.5	9.0	−1.7	0.4	8.9	−1.9	0.6	71.2

values < 0 are practically unpolluted (Müller, 1981). However, I_{geo} values up to 0.8 for Co imply unpolluted to moderately polluted sediments, I_{geo} values up to 1.5 for Cr imply moderate pollution, I_{geo} values up to 3.9 for Cu imply moderate to heavy pollution, and I_{geo} values up to 4.5 for Zn strongly imply heavy, extreme pollution. Therefore, all the streams in the study area are polluted with regard to the heavy elements investigated in this study considering their I_{geo} values, albeit with some level of nonpollution.

The CF values of the heavy metals in the sediments indicate low to very high contamination and vary as: As (0.3–335.5), Sb (0.2–64.8), Pb (0.5–64.4), Cd (0.7–63), Zn (0.4–34.5), Cu (0.1–21.9), Ni (0.2–10), Cr (0.2–4.2), and Co (0.0–2.6) (Table 3), decreasing in similar order as the EF values: As > Cd > Sb > Zn > Pb > Cu > Ni > Cr (Figure 2c). Among the studied streams, Alihoca and Gümüş streams have the highest CF values with the majority of sample points having CF values > 1. The samples show very high contamination for As, Sb, Pb, Cd, Zn, Cu, and Ni in the Alihoca and Gümüş streams. The highly contaminated sample points in these streams are located downstream close to the Pb-Zn-Au deposits and the contamination is likely due to discharge from metallic waste coming from the mines.

The PLI values varied from 0.5–6.0 with 30 out of the 53 total sample points showing PLI values > 1 (Table 3), implying that 57% of the sample points are contaminated by heavy metals to some degree. Higher PLI values indicate that As, Cd, Sb, and Pb are major contributors to the sediment pollution. As observed in the spatial distribution map of the PLI values, the most critical contamination of metals occurred in the southern and southwestern fringes of the study area where the Alihoca and Gümüş streams are located (Figure 3). The PLI for the four streams followed the order of Alihoca stream > Gümüş stream > Çakıt stream > Horoz stream. The overall metal pollution assessment indicates that the EF, I_{geo}, CF, and PLI values are very high in the Alihoca and Gümüş streams. Increasing urbanization in the area, especially in the southern and western parts, where the Alihoca and Gümüş streams are located, involves changes in land use activities apart from mining activities. These changes expose the streams to different contamination issues such as agrochemical inputs (fertilizers and herbicides) and domestic sewage.

3.4. Potential ecological risk assessment and comparison with sediment quality guidelines

To effectively assess the potential ecological risks associated with heavy metal pollution in the sediments around the

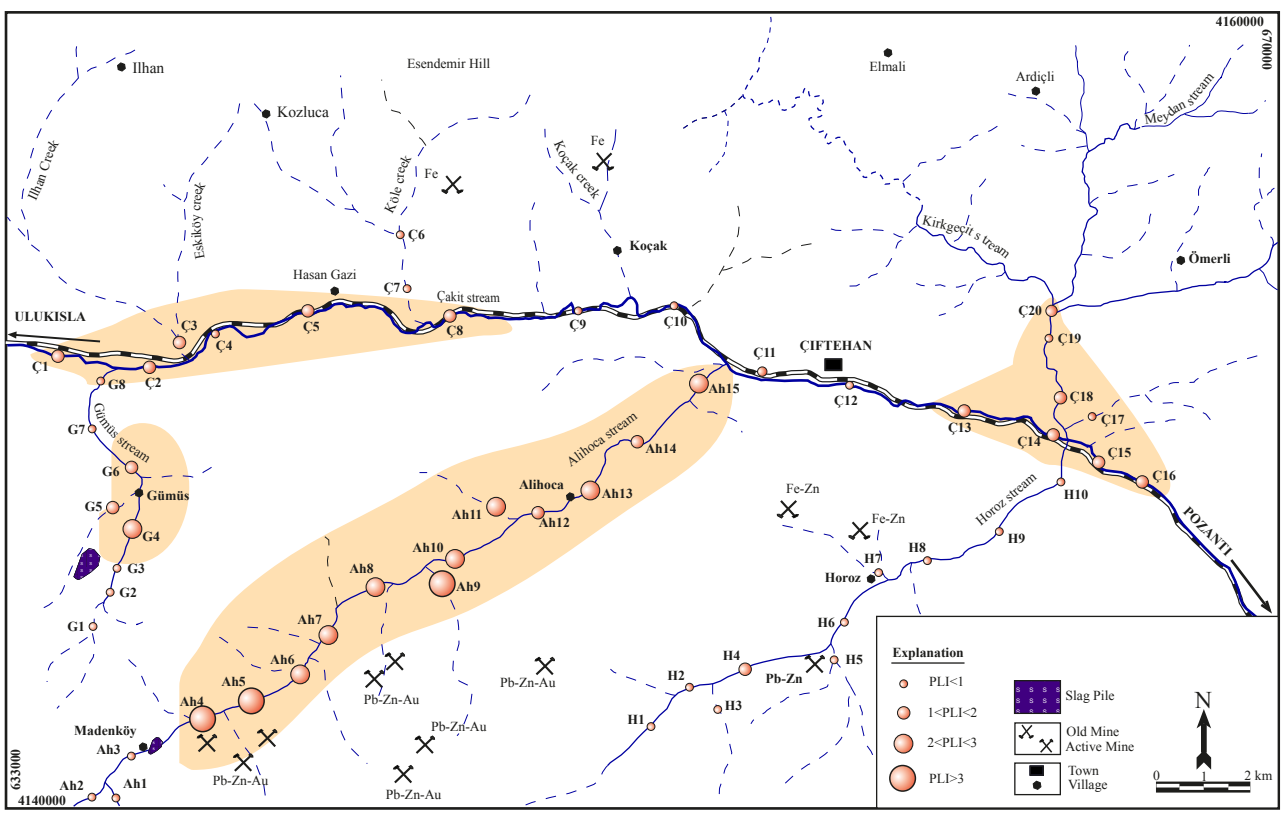

Figure 3. Spatial distribution of the pollution load index (PLI) values of heavy metals (As, Cd, Cr, Cu, Ni, Pb, Sb, Zn) in sediments of the Ulukışla Basin.

Ulukışla Basin, RI and SQGs were used in this study. The RI values of all the streams are presented in Table 3. The RI values range from 41–4298, implying very high potential ecological risk since they are mostly >40 (Bouzekri et al., 2019). The metals of critical concern in the potential ecological risk assessment are As, Cd, Sb, and Pb (Figure 4), as in the PLI assessment. Although other metals, including Cu, Zn, Ni, Cr, and Co have slightly lower RI values, they are still of concern since the RI values are all >40. In a spatial distribution map of the RI values, the highest potential ecological risk is observed in the Alihoca stream with some critical values at the Gümüş and Çakıt streams (Figure 5). This implies that aquatic organisms are at great risk in the study area.

The results of the potential ecological risk assessment are confirmed by the SQG values showing that concentrations of most of the heavy metals are above the threshold effect concentration (TEC) and the probable effect concentration (PEC) limits (Table 4). Sb, Cd, Zn, Pb, Cu, and As were lower than the TEC in 73.6%, 66%, 60.3%, 49.1%, 41.6%, and 24.5% of samples, respectively (Table 4). Cu, Cr, Pb, As, Cd, and Sb were between the TEC and PEC in 54.7%, 36.4%, 30.2%, 28.3%, and 22.7% of samples from all 4 streams, respectively (Table 4), showing that these metals may periodically affect aquatic organisms (Liao et al., 2017). However, Ni, Cr, As, Pb, Zn, and Cd exceeded the PEC in 83.1%, 62.3%, 47.2%, 20.8%, 20.8%, and 11.3% of samples, respectively (Table 4), implying that the concentration of these metals may frequently affect living organisms in the sediments (Varol, 2011; Liao et al., 2017). This risk becomes more dangerous in the Alihoca stream because most of the 15 samples collected in this stream have their Ni, As, Zn, Cr, and Cd concentrations exceeding the respective PEC values (Table 4). Such observation can be attributed to the intense discharge of metallic waste from the mines around the Alihoca stream.

3.5. Identification of metal pollution sources

In this study, Pearson's correlation matrix (PCM) and factor analysis (FA) using principal component analysis (PCA) were performed on the geochemical data. PCM and FA gave some useful constraints in understanding the sources and dynamics of pollutants in the sediments. From the PCM (Table 5), Al shows a strong positive correlation with only Co (r = 0.64) and moderate positive correlation with mud (r = 0.53), suggesting that Al and Co may have been adsorbed on the surfaces of argillaceous materials in the stream. Mn shows a moderate positive correlation with Zn (r = 0.56) and Cd (r = 0.58), suggesting that these metals are possibly from a common source and may be related to the mineralization in the area. Remarkably, Mo, Cu, Zn, As, and Sb display moderate to very strong positive correlations (r > 0.50–0.90) (Table 5), implying that these metals may be hydromorphically introduced into the stream in the sandbars. Although there is a

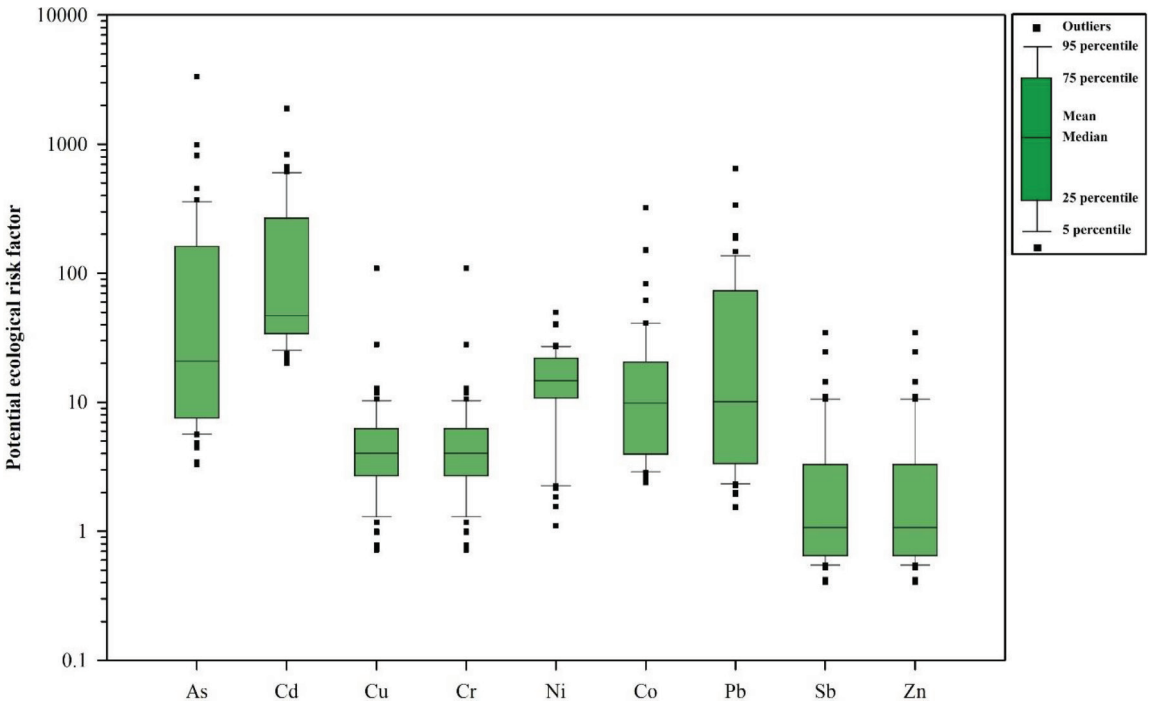

Figure 4. Box and whisker plot for the potential ecological risk factor of heavy metals (As, Cd, Cr, Cu, Ni, Pb, Sb, Zn) in sediments of the Ulukışla Basin.

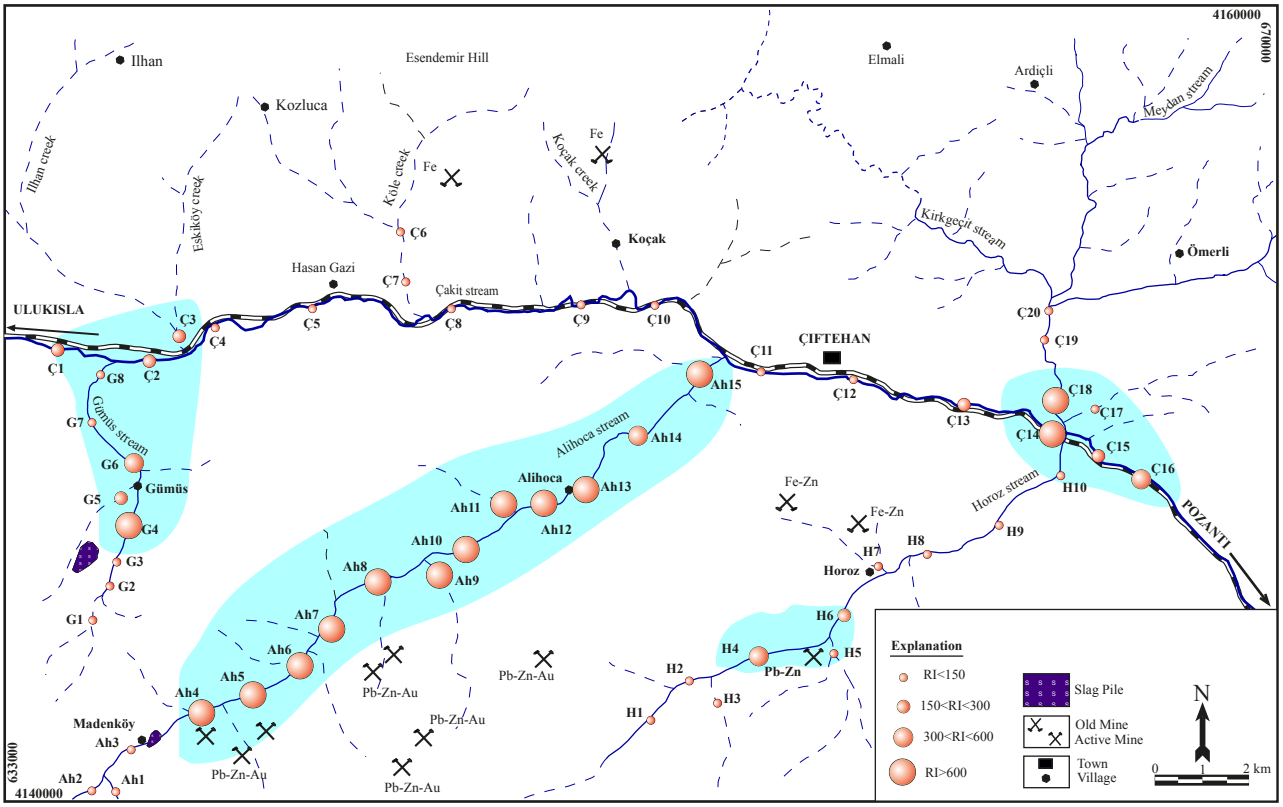

Figure 5. Spatial distribution of the potential ecological risk (RI) values of heavy metals (As, Cd, Cr, Cu, Ni, Pb, Sb, Zn) in sediments of the Ulukışla Basin.

significant correlation among these metals, it may not entirely imply that they all came from the same source. The source and pathway of these heavy metals can still be deciphered from interelement correlations. For instance, strong to very strong positive correlations between As and Zn (r = 0.71), As and Sb (r = 0.97), As and Cu (r = 0.97) strongly point to input from the polymetallic ores in the area. Mo, Cu, Zn, As, and Sb show moderate correlation (r ≥ 0.50) with total organic carbon (TOC), suggesting that sediment carbon sequestration is also responsible for their enrichment. Moreover, Co shows a very strong positive correlation with Ni (r = 0.92) and Cr (r = 0.84) (Table 5) implying a common geogenic source, particularly from weathering of the ophiolitic (Alihoca ophiolites) rocks in the area (Figure 1).

Four principal components (PCs) that explain 75.11% of the total variance of the geochemical data with eigenvalues > 1 were observed in the R-mode FA (Table 6). PC1 accounts for 27.60% of the total variance and significantly correlates with Cu, Pb, Zn, As, Mo, Sb, and TOC (Figure 6). These correlations agree with Pearson's correlation coefficient analysis (Table 5). The metals in PC1 were mainly derived from weathering and supergene alteration of base metal-rich mineralization (Yaylalı-Abanuz et al., 2012) along the streambeds and anthropogenic activities. Mining and agricultural activities are likely the main anthropogenic sources for the metal enrichment in PC1. PC1 showed a strong correlation with Pb, which may be due to anthropogenic input from mine slag piles that are widespread in the area. Jørgensen et al. (2005) and Shomar (2006) documented evidence of Zn and Cu enrichment in topsoil and attributed it to excessive agrochemical usage. The release of heavy metals from agricultural activities in the study area resulted in their accumulation in the stream sediments. Their distribution patterns are dependent on the contribution levels of pollution sources, stream environmental conditions, and sediment adsorption. The metal ionic potential values, climatic mechanical water cycle, and vertical direction metal leaching owing to grain size fraction of the sediments may also account for their distribution patterns in the sediments (Kalender and Uçar, 2013). PC2, constituting 22.83% of the total variance (Table 6), strongly correlates with Al, Ni, Co, Cr, and mud (Figure 6). These parameters are usually found in crustal materials and originate mainly from geological weathering (Guo et al., 2004). Weathering of magmatic rocks in the area may thus be accounting for their enrichment in the sediments. Therefore, PC2 may be coming from geogenic sources.

Table 4. Comparison between the heavy metal concentrations (mg/kg) in the Ulukışla Basin and sediment quality guidelines (SQGs), with the percentage of samples in each guideline.

	Parameter	As	Cd	Cr	Cu	Ni	Pb	Sb	Zn
SQGs	TEC	9.8	1.0	43.4	31.6	22.7	35.8	10.0	121.0
	PEC	33.0	5.0	111.0	149.0	48.6	128.0	35.0	459.0
Measured values	Min	4.3	0.2	17.8	6.5	15.0	9.6	0.2	36.4
	Max	4361.3	18.9	375.0	984.2	680.3	1287.9	507.6	3102.8
	Average	219.5	1.9	137.8	62.6	217.2	90.7	16.2	318.7
Çakıt stream	Samples < TEC	5	14	0	7	0	9	18	16
	TEC < Samples < PEC	8	6	5	13	0	8	2	3
	Samples > PEC	7	0	15	0	20	3	0	1
Alihoca stream	Samples < TEC	1	3	0	0	0	10	5	2
	TEC < Samples < PEC	2	6	5	13	0	3	8	3
	Samples > PEC	12	6	10	2	15	2	2	10
Gümüş stream	Samples < TEC	2	8	0	5	0	1	7	8
	TEC < Samples < PEC	3	0	0	3	0	3	1	0
	Samples > PEC	3	0	8	0	8	4	0	0
Horoz stream	Samples < TEC	5	10	6	10	2	6	9	6
	TEC < Samples < PEC	2	0	4	0	7	2	1	4
	Samples > PEC	3	0	0	0	1	2	0	0
Total	Samples < TEC	13 (24.5%)	35 (66.0%)	6 (11.3%)	22 (41.6%)	2 (3.7%)	26 (49.1%)	39 (73.6%)	32 (60.3%)
	TEC < Samples < PEC	15 (28.3%)	12 (22.7%)	14 (36.4%)	29 (54.7%)	7 (13.2%)	16 (30.2%)	12 (22.7%)	10 (18.9%)
	Samples > PEC	25 (47.2%)	6 (11.3%)	33 (62.3%)	2 (3.7%)	44 (83.1%)	11 (20.8%)	2 (3.7%)	11 (20.8%)

Table 5. Pearson's correlation matrix of the physicochemical parameters and heavy metals in the sediments of the Ulukışla Basin (correlation coefficients ≥ 0.60 are in bold and P > 0.01).

	Al	Fe	Mn	Mo	Cu	Pb	Zn	As	Cd	Sb	Co	Ni	Cr	TOC	Mud	$CaCO_3$
Al	1.00															
Fe	0.14	1.00														
Mn	0.27	–0.01	1.00													
Mo	–0.43	0.14	0.13	1.00												
Cu	–0.04	0.23	0.28	**0.60**	1.00											
Pb	0.07	0.17	0.05	0.14	0.36	1.00										
Zn	–0.31	0.04	0.56	0.51	0.57	0.10	1.00									
As	–0.17	0.22	0.32	**0.63**	**0.97**	0.37	**0.71**	1.00								
Cd	–0.34	–0.16	0.58	0.42	0.18	–0.10	**0.83**	0.31	1.00							
Sb	–0.11	0.25	0.21	0.59	**0.99**	0.38	0.56	**0.97**	0.13	1.00						
Co	**0.64**	0.06	0.30	–0.36	–0.04	0.14	–0.16	–0.08	–0.14	–0.10	1.00					
Ni	0.42	–0.03	0.29	–0.31	0.03	0.19	–0.07	0.02	–0.07	–0.01	**0.92**	1.00				
Cr	0.42	–0.06	0.36	–0.16	0.05	0.20	–0.04	0.01	0.05	–0.02	**0.84**	**0.92**	1.00			
TOC	–0.07	0.12	0.28	**0.66**	**0.63**	0.20	0.50	**0.68**	0.24	**0.62**	–0.10	–0.08	–0.02	1.00		
Mud	0.53	0.07	0.04	–0.17	0.25	0.36	–0.04	0.20	–0.23	0.23	0.38	0.29	0.24	0.29	1.00	
$CaCO_3$	–0.46	–0.44	0.06	0.16	–0.01	–0.07	0.24	0.06	0.37	0.00	–0.29	–0.10	–0.15	–0.07	–0.30	1.00

Table 6. Total variance explained after principal component analysis.

Component	Initial eigenvalues			Rotation sums of squared loadings		
	Total	% of variance	Cumulative %	Total	% of variance	Cumulative %
1	4.86	30.39	30.39	4.42	27.60	27.60
2	3.84	24.01	54.40	3.65	22.83	50.43
3	2.16	13.47	67.87	2.16	13.49	63.92
4	1.16	7.24	75.11	1.79	11.19	75.11
5	0.94	5.89	80.99			

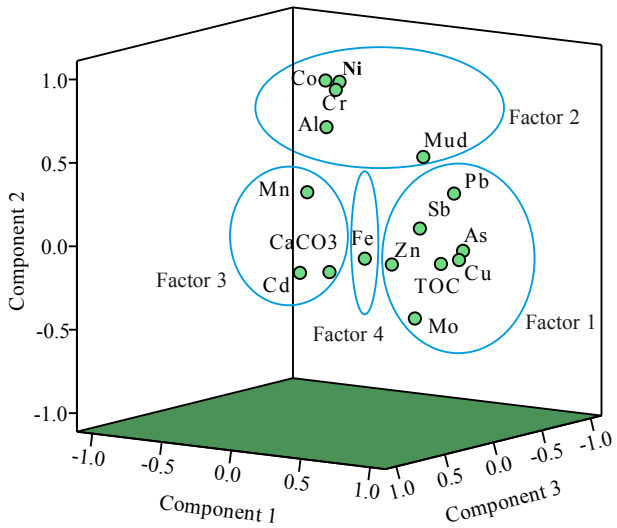

Figure 6. R-mode factor analysis plot of the physicochemical parameters and heavy metals in the studied sediments.

PC3 accounts for 13.49% of the total variance (Table 6) and loads strongly on Mn, Cd, and $CaCO_3$ (Figure 6). Such loadings may reflect the weathering of base metal deposits in carbonate rocks in the area. In addition, excessive use of pesticides and phosphate fertilizers in agricultural activities can cause Cd accumulation in the environment (Wang et al., 2015; Zhang et al., 2016). This implies that Cd loading might be partly coming from agrochemicals. PC4 accounts for 11.19% of the total variance and shows strong loading on only Fe but has minor positive loading on all the elements in PC3 (Figure 6). The positive loading of PC4 with Fe is likely from the dissolution of iron-bearing ores like Fe skarns (Horoz and Esendemirtepe Zn-Fe skarns) in the area (Kadıoğlu and Dilek, 2010; Kusçu, 2019). Fe may be present as carbonate in the sediments.

The results of the factor analysis were confirmed by hierarchical cluster analysis, which showed 4 main clusters (Figure 7). The first cluster involves Al, Pb, Co, Ni, Cr, and mud, which is similar to the loadings in PC2 in the factor analysis. This implies that cluster 1 reflects the weathering of the host rocks in the study area, as explained above. Cluster 2 is a subgroup of cluster 1 and involves only Fe, just like PC4 (Figure 7). Therefore, it shows positive loading on all the parameters in cluster 1 (Figure 7). Metals such as Pb and Fe usually adsorb onto mud and clay minerals as well as colloids of oxy-hydroxides in stream water (Potra et al., 2017). This causes them to be transported during surface run-off and resuspended from streambed sediments at high stream-flows (Hem, 1992). Moreover, increasing magnetic susceptibility on the mud surface may have favored the adsorption of Pb and Fe (Bouzekri et al., 2019). The association of Pb, Fe, and mud in clusters 1 and 2 is consistent with this interpretation. Cluster 3 is dominated by Mn, Mo, Cu, Zn, As, Cd, Sb, and TOC, similar to PC1 (Figure 7). Certainly, this element association is due to weathering, supergene alteration of base metal-rich mineralization (Yaylalı-Abanuz et al., 2012), and anthropogenic activities. Cluster 4 is a subgroup of cluster 3 and consists of only $CaCO_3$ (Figure 7). This cluster may point to the weathering of carbonate-bearing rocks and nonsulfide deposits (Hanilçi and Öztürk, 2011) in the study area. In all, the results of the cluster analysis corroborate well with that of the factor analysis.

3.6. Pb isotopic tracing in the sediments

The Pb isotopic ratios of the sediments range between 17.39 and 19.49 for $^{206}Pb/^{204}Pb$, 15.05 and 16.63 for $^{207}Pb/^{204}Pb$, 37.34 and 41.21 for $^{208}Pb/^{204}Pb$, and 1.09–1.29 for $^{206}Pb/^{207}Pb$ (Table 7). The Pb isotopic signatures of the sediments were compared to Pb isotope values of galena and sphalerite as well as slag pile from Madenköy, Horoz, and Gümüş villages in the study area, respectively, which show significant overlap (Table 7). This commonality gives a great deal of difficulty in discriminating between point sources of pollution of the stream sediments. It, therefore, requires taking into account other parameters such as the closeness of the sample points to the mining areas and transport of heavy metals into the streams. However, when one isotopic ratio is plotted against another, it can reveal general trends that can be used to identify Pb pollution

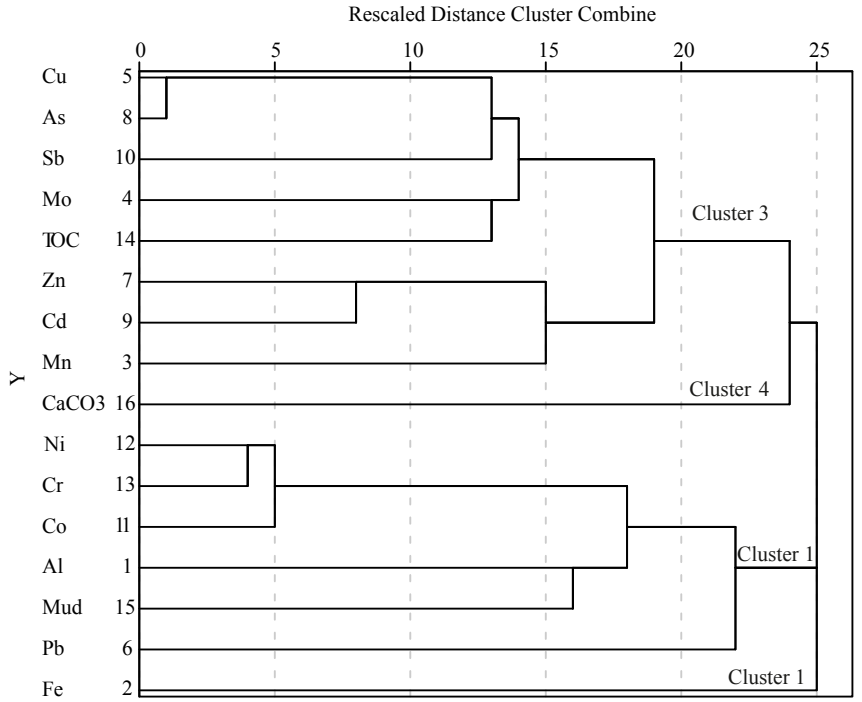

Figure 7. Dendrogram from hierarchical cluster analysis using average linkage between groups.

sources (Monna et al., 2000; Potra et al., 2017). In such plots, if the data form a cluster, a sole source of Pb can be invoked. However, if the data form several clusters, then multiple Pb sources can be inferred and linear trends imply mixed Pb sources (Hurst et al., 1996). The variations in Pb isotope compositions and metallic ores of the sediments point to numerous sources of Pb in the 4 streams under this study. The isotopic signature of the galena ore was significantly more radiogenic ($^{206}Pb/^{207}Pb$ up to 1.21) than the sphalerite ($^{206}Pb/^{207}Pb$ up to 1.19) and the slag pile ($^{206}Pb/^{207}Pb$ up to 1.10) (Table 7).

The Pb isotope compositions of the stream sediments define linear arrays forming 2 groups of Pb sources (Figure 8a). In Figure 6a, the majority of the samples overlap with the natural Pb source (first group), which includes galena and ultrapotassic rocks. Remarkably, there is a strong correlation between the 2 isotopic ratios (r = 0.72). The samples in the first group are dominated by those collected from the Alihoca and Çakıt streams with some samples from the Horoz and Gümüş streams (Figure 8a). It is therefore clear that extractable Pb in the stream sediments in group one was supplied by weathering of ore minerals such as galena and by ultrapotassic rocks that dominate the area. The second group includes samples from the Alihoca, Gümüş, and Çakıt streams, save for the Horoz stream, and overlap with another Pb source known as European gasoline (Figure 8a). Interestingly, the Pb isotopic ratios of the slag pile plot away from those of the stream sediments, albeit closer to samples from the Alihoca stream and may suggest limited contribution.

A plot of the $^{208}Pb/^{206}Pb$ and $^{206}Pb/^{207}Pb$ compositions shows a strong negative correlation (r = –0.78) between the 2 isotopic ratios and reveals another set of Pb sources for the studied sediments (Figure 8b). Two samples each from the Horoz and Çakıt streams overlap with the natural Pb source that contains galena, signifying that the weathering of galena mobilized a considerable amount of Pb in the stream sediments. One sample from the Çakıt stream falls in the field of Eastern Europe aerosols, 2 samples from the Alihoca stream and 1 sample from the Gümüş stream fall in the isotopic range of European gasoline, whereas 1 sample each from the Alihoca and Çakıt streams overlap with Kola Peninsula aerosols from Southern Russia (Figure 8b). The remaining samples have more radiogenic $^{208}Pb/^{206}Pb$ and $^{206}Pb/^{207}Pb$ ratios and plot away from the identified Pb sources (Figure 8b) and thus might be coming from other rare sources.

From the above evaluations, it appears that there are 2 major sources of Pb in the sediments of the Ulukışla Basin, which include geogenic and anthropogenic sources. To further understand the specific origin of Pb from these sources, the $^{206}Pb/^{207}Pb$ ratios and the bulk Pb content expressed as 1/Pb normalized values were plotted on a single diagram (Figure 9). This diagram shows high Pb pollution of the sediments in the Alihoca and Çakıt streams by geogenic sources with the resultant isotopic

Table 7. Pb isotopic compositions of the stream sediments in the Ulukışla Basin (included are Pb isotopic compositions of galena, sphalerite, and slag pile in the area).

Sample	Location	$^{207}Pb/^{204}Pb$	$^{206}Pb/^{204}Pb$	$^{208}Pb/^{204}Pb$	$^{206}Pb/^{207}Pb$	$^{208}Pb/^{207}Pb$	$^{208}Pb/^{206}Pb$	$^{206}Pb/^{207}Pb$
Galena	Madenköy	15.734	18.897	39.017	1.201	2.480	2.065	1.201
Galena	Madenköy	15.702	18.975	39.158	1.208	2.494	2.064	1.208
Galena	Madenköy	15.725	19.030	39.256	1.210	2.496	2.063	1.210
Sphalerite	Horoz	15.688	18.648	38.858	1.189	2.477	2.084	1.189
SL1	Gümüş slag pile	15.882	17.487	39.243	1.101	2.471	2.244	1.101
Ah1	Alihoca stream	15.979	17.918	38.484	1.121	2.408	2.148	1.121
Ah2		15.669	18.408	38.648	1.175	2.467	2.099	1.175
Ah4		16.527	18.527	39.527	1.121	2.392	2.133	1.121
Ah5		15.878	18.492	41.212	1.165	2.596	2.229	1.165
Ah6		16.441	18.232	39.852	1.109	2.424	2.186	1.109
Ah7		15.396	19.096	38.862	1.240	2.524	2.035	1.240
Ah8		15.945	18.086	41.058	1.134	2.575	2.270	1.134
Ah9		15.782	19.087	40.602	1.209	2.573	2.127	1.209
Ah10		16.473	17.924	39.061	1.088	2.371	2.179	1.088
Ah11		15.052	18.689	38.616	1.242	2.566	2.066	1.242
Ah12		16.074	17.695	38.975	1.101	2.425	2.203	1.101
Ah13		15.452	18.880	39.246	1.222	2.540	2.079	1.222
Ç3	Çakıt stream	15.579	18.714	39.484	1.201	2.534	2.110	1.201
Ç5		15.762	17.390	37.733	1.103	2.394	2.170	1.103
Ç13		16.224	18.618	38.882	1.148	2.397	2.088	1.148
Ç14		15.456	17.910	39.380	1.159	2.548	2.199	1.159
Ç15		14.951	18.566	37.343	1.242	2.498	2.011	1.242
Ç16		14.941	18.468	37.614	1.236	2.518	2.037	1.236
Ç18		15.883	18.298	39.655	1.152	2.497	2.167	1.152
G3	Gümüş stream	15.082	19.487	39.602	1.292	2.626	2.032	1.292
G4		16.627	18.427	38.927	1.108	2.341	2.113	1.108
G6		15.482	18.867	39.602	1.219	2.558	2.099	1.219
G8		15.682	17.525	37.561	1.118	2.395	2.143	1.118
H5	Horoz stream	15.536	18.884	38.246	1.215	2.462	2.025	1.215
H6		15.495	17.985	38.691	1.161	2.497	2.151	1.161
H10		15.179	17.714	38.184	1.167	2.515	2.155	1.167

signature. Thus, this pollution may be related to weathering and dissolution of ultrapotassic rocks and galena from magmatic related ore deposits in the area, which have a similar isotopic signature. The $^{206}Pb/^{207}Pb$ ratios and 1/Pb normalized values also revealed that in general, a trend of increasing 1/Pb normalized values was accompanied by a shift toward lower isotopic ratios because of a large contribution from anthropogenic (excess) Pb (Figure 9). The anthropogenic Pb may have originated from slag piles in the area due to mining activities but other anthropogenic sources could also be inferred. This Pb pollution source affected samples from all 4 streams but predominantly from the Alihoca and Gümüş streams (Figure 9). In conclusion, Pb isotopic signatures of the sediments define a simple 3-component mixing model that involves a background component (natural Pb), Pb derived from ore deposits in the area, and Pb from slag piles (Figure 8).

4. Conclusions

This study provides new geochemical data of heavy metals in stream sediments around the south-central Taurides (Ulukışla Basin), Niğde. The results indicate that the general order of heavy metal pollution is in the

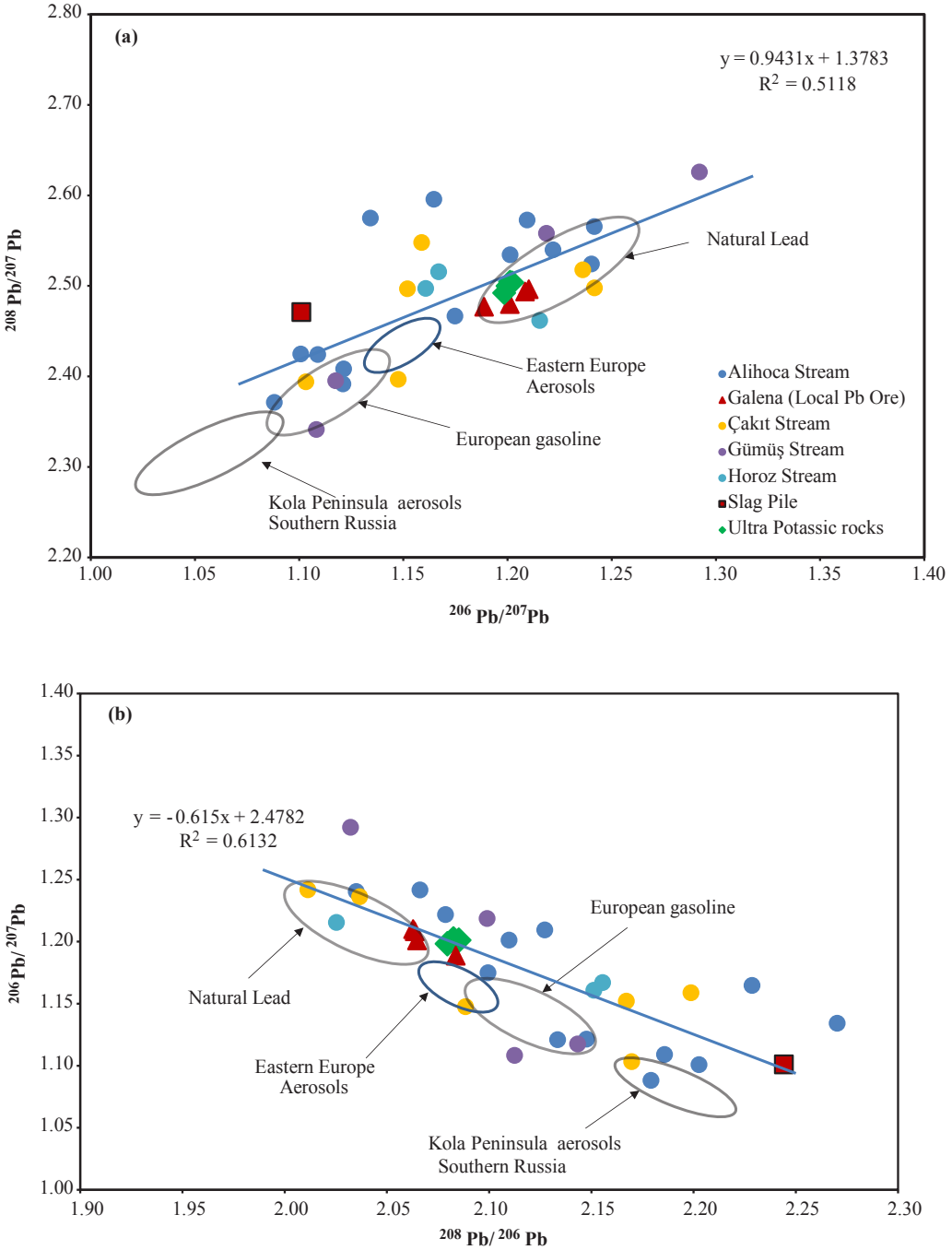

Figure 8. Plots of (a) $^{206}Pb/^{207}Pb$ vs. $^{208}Pb/^{207}Pb$ and (b) $^{208}Pb/^{206}Pb$ vs. $^{206}Pb/^{207}Pb$ in the sediments and the potential source materials [data for Eastern Europe and Kola Peninsula aerosols were taken from Bollhöfer and Rosman (2001); European gasoline from Komárek et al., 2008; Ultra potassic rocks from Alpaslan et al., 2006].

order of As > Cd > Sb > Zn > Pb > Cu > Ni > Cr > Co for all the pollution indices. As, Cd, Sb, Zn, Cu, Pb, and Ni are elements of critical concern. From the potential ecological risk assessment, the sediments show very high ecological risk with As, Cd, Sb, and Pb as the main contributors. Using the sediment quality guidelines, Ni, Cr, As, Pb, Zn, and Cd exceeded the probable effect concentrations in almost all the samples, suggesting that the concentration of these metals is likely to affect aquatic living organisms in the sediments. Sediment

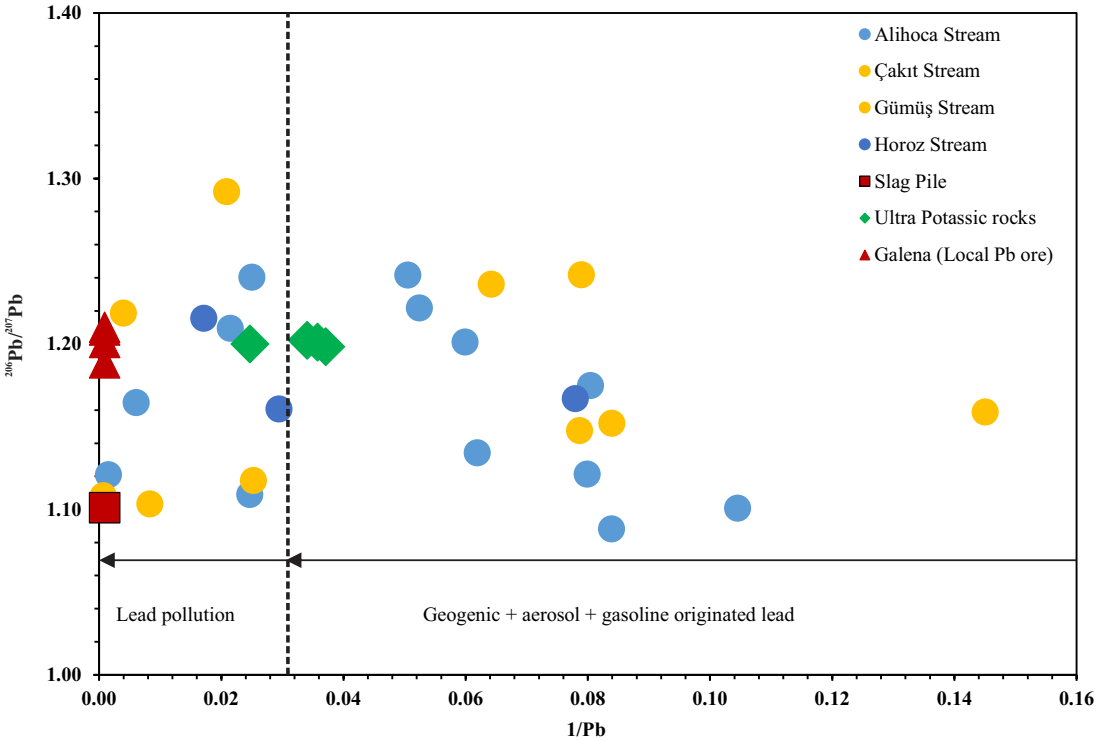

Figure 9. 1/Pb normalized values vs. $^{206}Pb/^{207}Pb$ ratios showing the sources and degrees of contamination of the stream sediments.

pollution is higher in Alihoca, Horoz, and Gümüş streams than the Çakıt stream. Multivariate statistical analyses indicate that the cluster of metals involving Cu, Zn, As, Cd, Mo, and Sb was derived from anthropogenic sources (mining and agriculture), whereas Al, Mn, Ni, Co, and Cr may be coming from geogenic sources. Pb isotopic tracing indicates that the influx of Pb in the streams is dominated by Pb sourced from weathering and dissolution of potassic rocks and galena from the Pb-Zn-Au deposits in the area. Anthropogenic input from slag piles owing to historic mining in the area also contributed to the accumulation of Pb in the stream sediments. These results call for the need for an environmental monitoring scheme to support the development of an efficient remediation strategy that will help minimize local pollution of streams in the area.

Acknowledgments

This research was financially supported in part by the Scientific Research Projects office of Niğde Ömer Halisdemir University (Project no. FEB 2011/10). Emmanuel Daanoba Sunkari acknowledges the continuous support from the Scientific and Technological Research Council of Turkey (TÜBİTAK) as a doctoral fellow of BIDED 2215 Graduate Scholarship Program for International Students. The editor and the 3 anonymous reviewers are also greatly appreciated for the good reviews that improved the quality of this paper.

References

Ahmad MK, Islam S, Rahman S, Haque MR, Islam MM (2010). Heavy metals in water, sediment and some fishes of Buriganga River, Bangladesh. International Journal of Environmental Research 4: 321-332.

Akçay M (1995). Fluid inclusions and chemistry of tourmalines from the Gümüşler Sb-Hg±W deposits of the Niğde Massif (Central Turkey). Chemie der Erde 55: 225-236.

Alpaslan M, Boztuğ D, Frei R, Temel A, Kurt MA (2006). Geochemical and Pb–Sr–Nd isotopic composition of the ultrapotassic volcanic rocks from the extension-related Çamardı-Ulukışla basin, Niğde Province, Central Anatolia, Turkey. Journal of Asian Earth Sciences 27(5): 613-627.

Andrews S, Sutherland RA (2004). Cu, Pb and Zn contamination in Nuuanu watershed, Oahu, Hawaii. Science of the Total Environment 324(1-3): 173-182.

Bollhöfer A, Rosman KJR (2001). Isotopic source signatures for atmospheric lead: the Northern Hemisphere. Geochimica et Cosmochimica Acta 65(11): 1727-1740.

Bouzekri S, El Hachimi ML, Touach N, El Fadili H, El Mahi M (2019). The study of metal (As, Cd, Pb, Zn and Cu) contamination in superficial stream sediments around of Zaida mine (High Moulouya-Morocco). Journal of African Earth Sciences 154: 49-58.

Cheng H, Hu Y (2010). Lead (Pb) isotopic fingerprinting and its applications in lead pollution studies in China: a review. Environmental Pollution 158(5): 1134-1146.

Clark M, Robertson A (2002). The role of the Early Tertiary Ulukisla Basin, southern Turkey, in suturing of the Mesozoic Tethys ocean. Journal of the Geological Society 159(6): 673-690.

Das A, Patel SS, Kumar R, Krishna KVSS, Dutta S et al. (2018). Geochemical sources of metal contamination in a coal mining area in Chhattisgarh, India using lead isotopic ratios. Chemosphere 197: 152-164.

Demirak A, Yilmaz F, Tuna AL, Ozdemir N (2006). Heavy metals in water, sediment and tissues of Leuciscus cephalus from a stream in southwestern Turkey. Chemosphere 63(9): 1451-1458.

Dilek Y, Thy P, Hacker B, Grundvig S (1999). Structure and petrology of Tauride ophiolites and mafic dyke intrusions (Turkey): implications for the Neotethyan ocean. Geological Society of America Bulletin 111: 1192-1216.

Eker ÇS, Sipahi F, Özkan Ö, Gümüş MK (2017). Evaluation of potentially toxic element contents and Pb isotopic compositions in Ankara Stream sediments within an urban catchment in central Turkey. Environmental earth sciences 76(19): 647. doi: 10.1007/s12665-017-6985-y

Ettler V, Mihaljevič M, Šebek O, Molek M, Grygar T et al. (2006). Geochemical and Pb isotopic evidence for sources and dispersal of metal contamination in stream sediments from the mining and smelting district of Příbram, Czech Republic. Environmental Pollution 142(3): 409-417.

Gaur VK, Gupta SK, Pandey SD, Gopal K, Misra V (2005). Distribution of heavy metals in sediment and water of river Gomti. Environmental monitoring and assessment 102(1-3): 419-433.

Guitián F, Carballas T (1976). Técnicas de análisis de suelos. Ed. Pico Sacro. Santiago, p. 288.

Guo J, Rahn KA, Zhuang G (2004). A mechanism for the increase of pollution elements in dust storms in Beijing. Atmospheric Environment 38(6): 855-862.

Guo X, Jie X, Hasi T, Liu S, Hua D et al. (2009). Effects of lucerne hay with higher content of trace elements in diets on performance of dorper sheep. Journal of Domestic Animal Ecology 30: 29-33 (in Chinese).

Hakanson L (1980). An ecological risk index for aquatic pollution control. A sedimentological approach. Water Research 14(8): 975-1001.

Hanilçi (2013). Geological and geochemical evolution of the Bolkardaği bauxite deposits, Karaman, Turkey: transformation from shale to bauxite. Journal of Geochemical Exploration 133:118-137.

Hanilçi N (2019). Bauxite deposits of Turkey. In: Pirajno F, Dönmez C Şahin MB (ed) Mineral Resources of Turkey. Modern Approaches in Solid Earth Sciences. Springer Nature Switzerland 16(15):681-730.

Hanilçi N, Öztürk H (2011). Geochemical/isotopic evolution of Pb–Zn deposits in the Central and Eastern Taurides, Turkey. International Geology Review 53(13): 1478-1507.

Hanken NM, Bjørlykke K, Nielsen JK (2015). Carbonate sediments. In: Petroleum Geoscience. Springer, Berlin, Heidelberg, pp. 151-216.

Hem JD (1992). Manganese-bearing Precipitates Formed from Water in Pinal Creek Basin, Arizona. Abstracts of Papers. American Chemical Society. National Meeting 203, GEOC.

Hurst RW, Davis TE, Chinn BD (1996). The lead fingerprints of gasoline contamination. Environmental Science and Technology 30: 304A-307A.

Hyun S, Lee CH, Lee T, Choi JW (2007). Anthropogenic contributions to heavy metal distributions in the surface sediments of Masan Bay, Korea. Marine Pollution Bulletin 54(7): 1059. doi: 10.1016/j.marpolbul.2007.02.013.

Jiang Y, Chao S, Liu J, Yang Y, Chen Y et al. (2017). Source apportionment and health risk assessment of heavy metals in soil for a township in Jiangsu Province, China. Chemosphere 168: 1658-1668.

Jørgensen N, Laursen J, Viksna A, Pind N, Holm PE (2005). Multi-elemental EDXRF mapping of polluted soil from former horticultural land. Environment International 31(1): 43-52.

Kadioglu YK, Dilek Y (2010). Structure and geochemistry of the adakitic Horoz granitoid, Bolkar Mountains, south-central Turkey, and its tectonomagmatic evolution. International Geology Review 52(4-6): 505-535.

Kaiser HF (1960). The application of electronic computers to factor analysis. Educational and Psychological Measurement 20(1): 141-151.

Kalelioğlu Ö, Zorlu K, Kurt MA, Gül M, Güler C (2009). Delineating compositionally different dykes in the Ulukışla basin (Central Anatolia, Turkey) using computer-enhanced multi-spectral remote sensing data. International Journal of Remote Sensing 30(11): 2997-3011.

Kalender L, Uçar SÇ (2013). Assessment of metal contamination in sediments in the tributaries of the Euphrates River, using pollution indices and the determination of the pollution source, Turkey. Journal of Geochemical Exploration 134: 73-84.

Keskin Ş (2012). Distribution and accumulation of heavy metals in the sediments of Akkaya Dam, Niğde, Turkey. Environmental Monitoring and Assessment 184(1): 449-460.

Keskin Ş, Şener M, Şener MF, Öztürk MZ (2017). Depositional environment characteristics of Ulukışla Evaporites, Central Anatolia, Turkey. Carbonates and Evaporates 32(2): 231-241.

Kirat G, Aydin N (2018). Investigation of metal pollution in Moryayla (Erzurum) and surrounding stream sediments, Turkey. International Journal of Environmental Science and Technology 15(10): 2229-2240.

Kocak K, Zedef V, Kansun G (2011). Magma mixing/mingling in the Eocene Horoz (Niğde) granitoids, Central southern Turkey: evidence from mafic microgranular enclaves. Mineralogy and Petrology 103(1-4): 149-167.

Komárek M, Ettler V, Chrastný V, Mihaljevič M (2008). Lead isotopes in environmental sciences: a review. Environment International 34(4): 562-577. doi: 10.1016/j.envint.2007.10.005.

Kumar B, Singh UK (2018). Source apportionment of heavy metals and their ecological risk in a tropical river basin system. Environmental Science and Pollution Research 25(25): 25443-25457.

Kuşcu İ (2019). Skarns and Skarn Deposits of Turkey. In Mineral Resources of Turkey. Cham, Switzerland: Springer, pp. 283-336).

Kuşcu İ, Tosdal RM, Gencalioğlu-Kuşcu G, Friedman R, Ullrich TD (2013). Late Cretaceous to Middle Eocene magmatism and metallogeny of a portion of the Southeastern Anatolian orogenic belt, East-Central Turkey. Economic Geology 108(4): 641-666.

Larrose A, Coynel A, Schäfer J, Blanc G, Massé L et al. (2010). Assessing the current state of the Gironde Estuary by mapping priority contaminant distribution and risk potential in surface sediment. Applied Geochemistry 25(12): 1912-1923.

Lermi A (2016). Pollution Evaluation of Heavy Metals in Sediments from the Çakit Stream, Ulukişla (Niğde), Turkey. International Multidisciplinary Scientific GeoConference: SGEM: Surveying Geology & mining Ecology Management 1: 491-497.

Lermi A, Ertan G (2019). Hydrochemical and isotopic studies to understand quality problems in groundwater of the Niğde Province, Central Turkey. Environmental Earth Sciences 78(12): 365. doi: 10.1007/s12665-019-8365-2.

Lermi A, Sönmez M, Aydin F (2016). Mineralogy and Geochemistry of the Kiziltepe (Çamardi-Niğde) Mn Prospect in Central Anatolia, Turkey. International Multidisciplinary Scientific GeoConference: SGEM: Surveying Geology & Mining Ecology Management 1: 421-428.

Lermi, A (2009). Gümüşköy-Maden (Ulukışla-Niğde) Bölgesindeki Toprak, Su ve Bitkilerde Maden Atıklarından Kaynaklanan Ağır Metal Kirlilik Düzeyleri, 1. Tıbbi Jeoloji Çalıştayı, Bildiriler Kitabı. Ürgüp, Nevşehir, Turkey 1: 94-109 (in Turkish).

Liao J, Chen J, Ru X, Chen J, Wu H et al. (2017). Heavy metals in river surface sediments affected with multiple pollution sources, South China: Distribution, enrichment and source apportionment. Journal of Geochemical Exploration 176: 9-19.

Lin C, Yu R, Hu G, Yang Q, Wang X (2016). Contamination and isotopic composition of Pb and Sr in offshore surface sediments from Jiulong River, Southeast China. Environmental Pollution 218: 644-650.

Liu JT, Hsu RT, Yang RJ, Wang YP, Wu H et al. (2018). A comprehensive sediment dynamics study of a major mud belt system on the inner shelf along an energetic coast. Scientific Reports 8(1):4229. doi: 10.1038/s41598-018-22696-w.

MacDonald DD, Ingersoll CG, Berger TA (2000). Development and evaluation of consensus-based sediment quality guidelines for freshwater ecosystems. Archives of Environmental Contamination and Toxicology 39: 20-31.

Monna F, Hamer K, Lévêque J, Sauer M (2000). Pb isotopes as a reliable marker of early mining and smelting in the Northern Harz province (Lower Saxony, Germany). Journal of Geochemical Exploration 68(3): 201-210.

Mucha AP, Vasconcelos MTSD, Bordalo AA (2003). Macrobenthic community in the Douro Estuary: relations with trace metals and natural sediment characteristics. Environmental Pollution 121: 169-180.

Müller G (1969). Index of geoaccumulation in sediments of the Rhine River. Geojournal 2: 108-118.

Müller G (1981). Die Schwermetallbelstung der sedimente des Neckars und seiner Nebenflusse: eine Bestandsaufnahme. Chemiker-Zeitung 105: 157-164 (in German).

Omwene PI, Öncel MS, Çelen M, Kobya M (2018). Heavy metal pollution and spatial distribution in surface sediments of Mustafakemalpaşa stream located in the world's largest borate basin (Turkey). Chemosphere 208: 782-792.

Orani AM, Vassileva E, Renac C, Schmidt S, Angelidis MO et al. (2019). First assessment on trace elements in sediment cores from Namibian coast and pollution sources evaluation. Science of the Total Environment 669: 668-682.

Öztürk H (1997). Manganese deposits in Turkey: distribution, types and tectonic setting. Ore Geology Reviews 12(3): 187-203.

Pobi KK, Satpati S, Dutta S, Nayek S, Saha RN et al. (2019). Sources evaluation and ecological risk assessment of heavy metals accumulated within a natural stream of Durgapur industrial zone, India, by using multivariate analysis and pollution indices. Applied Water Science 9(3): 58.

Potra A, Dodd JW, Ruhl LS (2017). Distribution of trace elements and Pb isotopes in stream sediments of the Tri-State mining district (Oklahoma, Kansas, and Missouri), USA. Applied Geochemistry 82: 25-37.

Shomar BH (2006). Trace elements in major solid-pesticides used in the Gaza Strip. Chemosphere 65(5): 898-905.

Sin SN, Chua H, Lo W, Ng LM (2001). Assessment of heavy metal cations in sediments of Shing Mun River, Hong Kong. Environment International 26(5-6): 297-301.

Singh KP, Mohan D, Singh VK, Malik A (2005). Studies on distribution and fractionation of heavy metals in Gomti river sediments—a tributary of the Ganges, India. Journal of Hydrology 312(1-4): 14-27.

Sun J, Hu G, Yu R, Lin C, Wang X et al. (2017). Human health risk assessment and source analysis of metals in soils along the G324 Roadside, China, by Pb and Sr isotopic tracing. Geoderma 305: 293-304.

Sunkari ED, Appiah-Twum M, Lermi A (2019). Spatial distribution and trace element geochemistry of laterites in Kunche area: Implication for gold exploration targets in NW, Ghana. Journal of African Earth Sciences 103519. doi: 10.1016/j.jafrearsci.2019.103519.

Tomlinson DL, Wilson JG, Harris CR, Jeffrey DW (1980). Problems in the assessment of heavy-metal levels in estuaries and the formation of a pollution index. Helgoländer Meeresuntersuchungen 33(1): 566-575.

Tuna AL, Yilmaz F, Demirak A, Ozdemir N (2007). Sources and distribution of trace metals in the Saricay stream basin of southwestern Turkey. Environmental Monitoring and Assessment 125(1-3): 47-57.

Turekian KK, Wedepohl KH (1961). Distribution of the elements in some major units of the earth's crust. Geological Society of America Bulletin 72(2): 175-192.

Ustaoğlu F, Tepe Y (2019). Water quality and sediment contamination assessment of Pazarsuyu Stream, Turkey using multivariate statistical methods and pollution indicators. International Soil and Water Conservation Research 7(1): 47-56.

Varol M (2011). Assessment of heavy metal contamination in sediments of the Tigris River (Turkey) using pollution indices and multivariate statistical techniques. Journal of Hazardous Materials 195: 355-364.

Vrhovnik, P, Smuc, NR, Dolenec, T, Serafimovski, T, Dolenec, M (2013). Impact of Pb-Zn mining activity on surficial sediments of Lake Kalimanci (FYR Macedonia). Turkish Journal of Earth Sciences 22(6): 996-1009.

Wang L, Cui X, Cheng H, Chen F, Wang J et al. (2015). A review of soil cadmium contamination in China including a health risk assessment. Environmental Science and Pollution Research 22(21): 16441-16452.

Yalcin MG, Aydin O, Elhatip H (2008a). Heavy metal contents and the water quality of Karasu Creek in Niğde, Turkey. Environmental Monitoring and Assessment 137(1-3): 169. doi 10.1007/s10661-007-9737-8.

Yalcin MG, Narin I, Soylak M (2007). Heavy metal contents of the Karasu creek sediments, Niğde, Turkey. Environmental Monitoring and Assessment 128(1-3): 351-357.

Yalcin MG, Narin I, Soylak M (2008b). Multivariate analysis of heavy metal contents of sediments from Gümüşler creek, Niğde, Turkey. Environmental Geology 54(6): 1155-1163.

Yaylalı-Abanuz G, Tüysüz N, Akaryalı E (2012). Soil geochemical prospection for gold deposit in the Arzular area (NE Turkey). Journal of Geochemical Exploration 112: 107-117.

Yu R, Hu G, Lin C, Yang Q, Zhang C et al. (2017). Contamination of heavy metals and isotopic tracing of Pb in intertidal surface sediments of Jinjiang River Estuary, SE China. Applied Geochemistry 83: 41-49.

Zango MS, Sunkari ED, Abu M, Lermi A (2019). Hydrogeochemical controls and human health risk assessment of groundwater fluoride and boron in the semi-arid north east region of Ghana. Journal of Geochemical Exploration 106363. doi: 10.1016/j.gexplo.2019.106363.

Zhang J, Liu CL (2002). Riverine composition and estuarine geochemistry of particulate metals in China—weathering features, anthropogenic impact and chemical fluxes. Estuarine, Coastal and Shelf Science 54(6): 1051-1070.

Zhang Z, Juying L, Mamat Z, QingFu Y (2016). Sources identification and pollution evaluation of heavy metals in the surface sediments of Bortala River, Northwest China. Ecotoxicology and Environmental Safety 126: 94-101.

Zhang Z, Lu Y, Li H, Tu Y, Liu B et al. (2018). Assessment of heavy metal contamination, distribution and source identification in the sediments from the Zijiang River, China. Science of the Total Environment 645: 235-243.

Zhao D, Wan S, Yu Z, Huang J (2015). Distribution, enrichment and sources of heavy metals in surface sediments of Hainan Island rivers, China. Environmental Earth Sciences 74: 5097-5110.

Zuluaga MC, Norini G, Lima A, Albanese S, David CP et al. (2017). Stream sediment geochemical mapping of the Mount Pinatubo-Dizon Mine area, the Philippines: Implications for mineral exploration and environmental risk. Journal of Geochemical Exploration 175: 18-35.